Contraction of Magnetized Rotating Clouds and Outflows

Kohji Tomisaka

with collaborators: M. N. Machida (Kyoto U.), K. Saigo (NAOJ), T. Matsumoto (Hosei U.), Hanawa (Chiba U.)

国立天文台

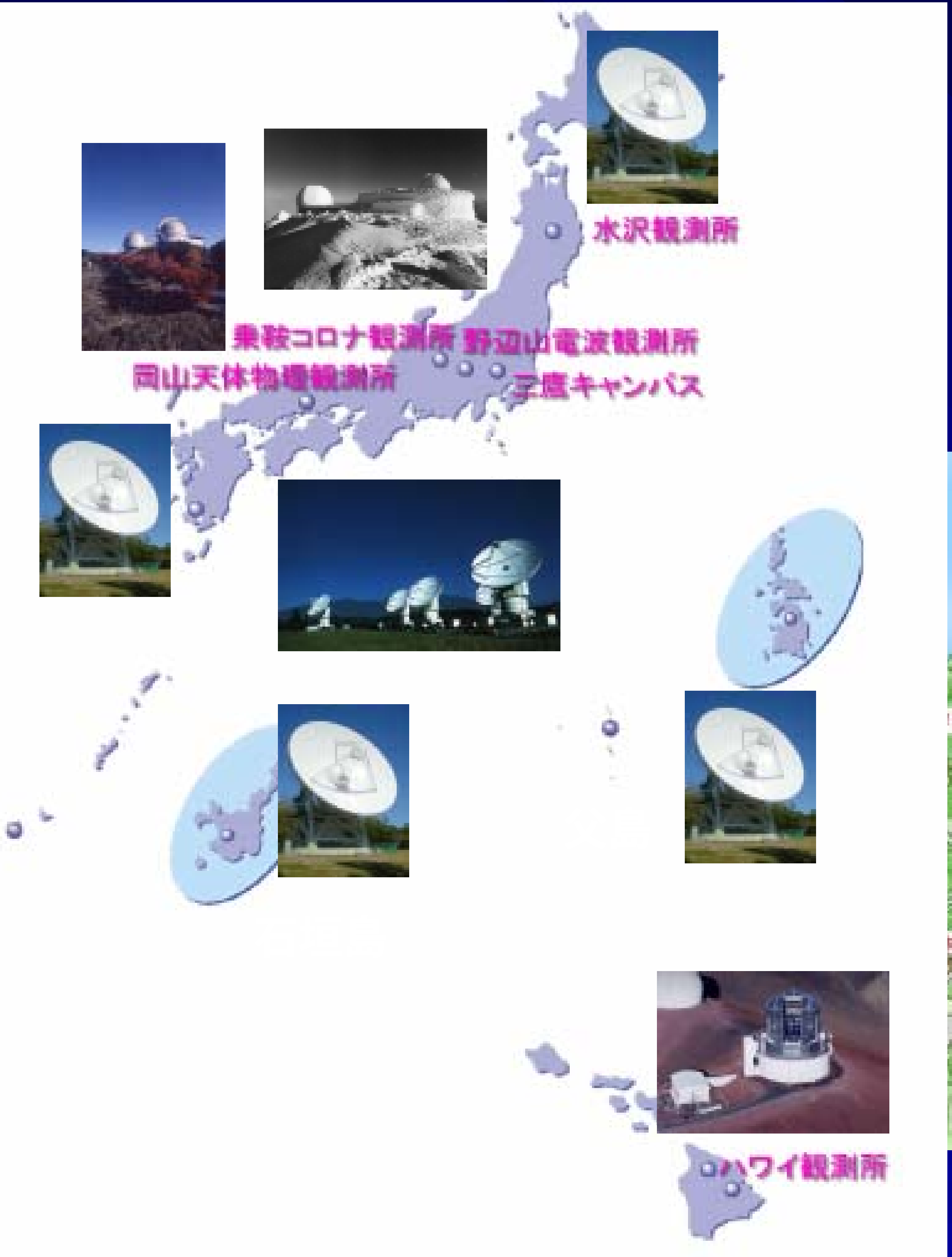
水沢観測所
乗鞍コロナ観測所
野辺山電波観測所
岡山天体物理観測所
三鷹キャンパス
ハワイ観測所


自動光電子午環
太陽フレア望遠鏡
赤外シミュレータ
TAMA 重力波実験棟
天文台歴史館
展示室
太陽系ウォーキング
計算機センター
50㌢反射望遠鏡
第一赤道儀室
食堂・売店

Taurus Molecular Cloud

^{13}CO

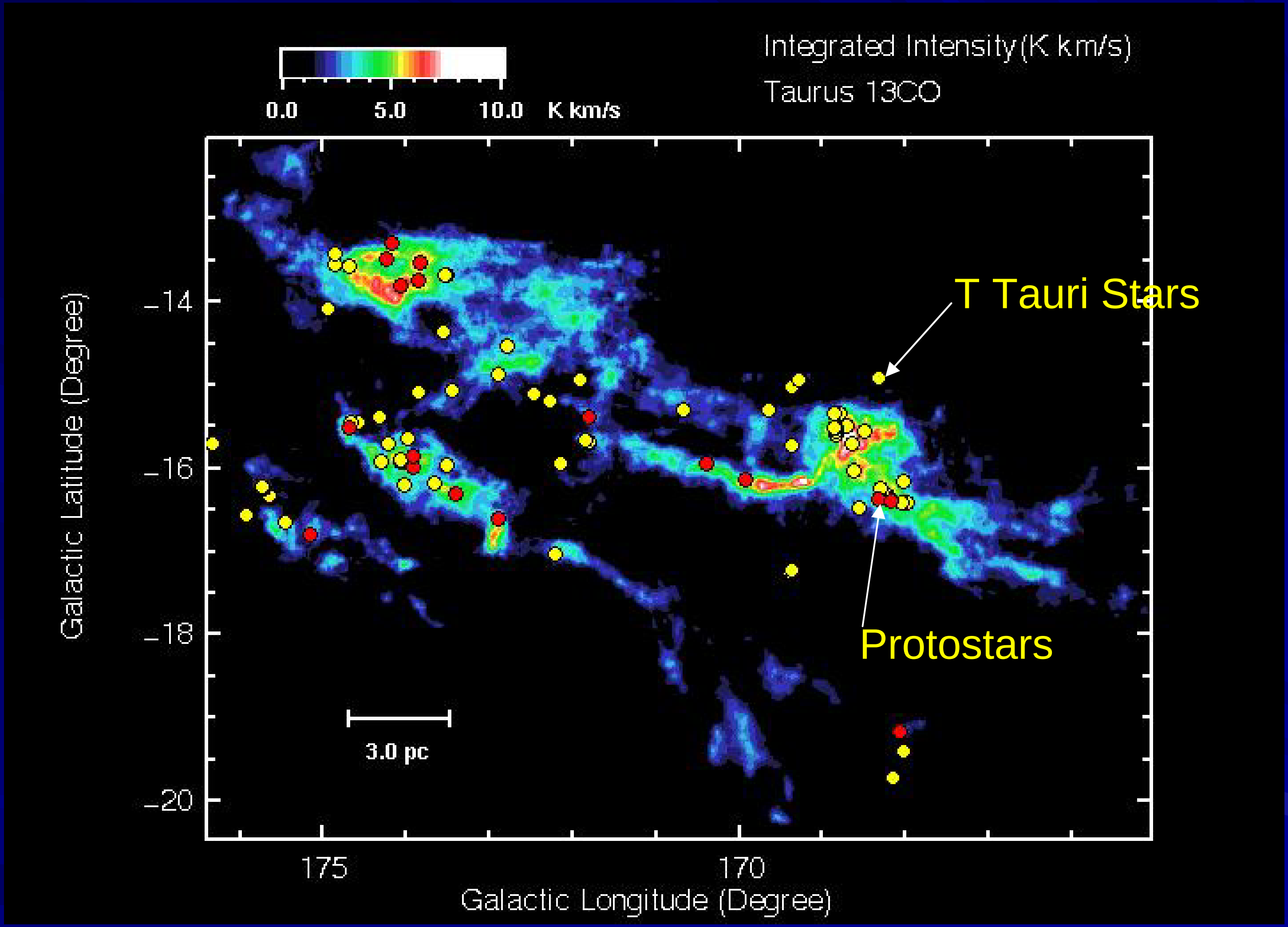

^{13}CO map of Taurus molecular cloud observed by Nagoya 4m radio telescope.

Star Formation in Molecular Cloud

Molecular Cores

$C^{18}O$

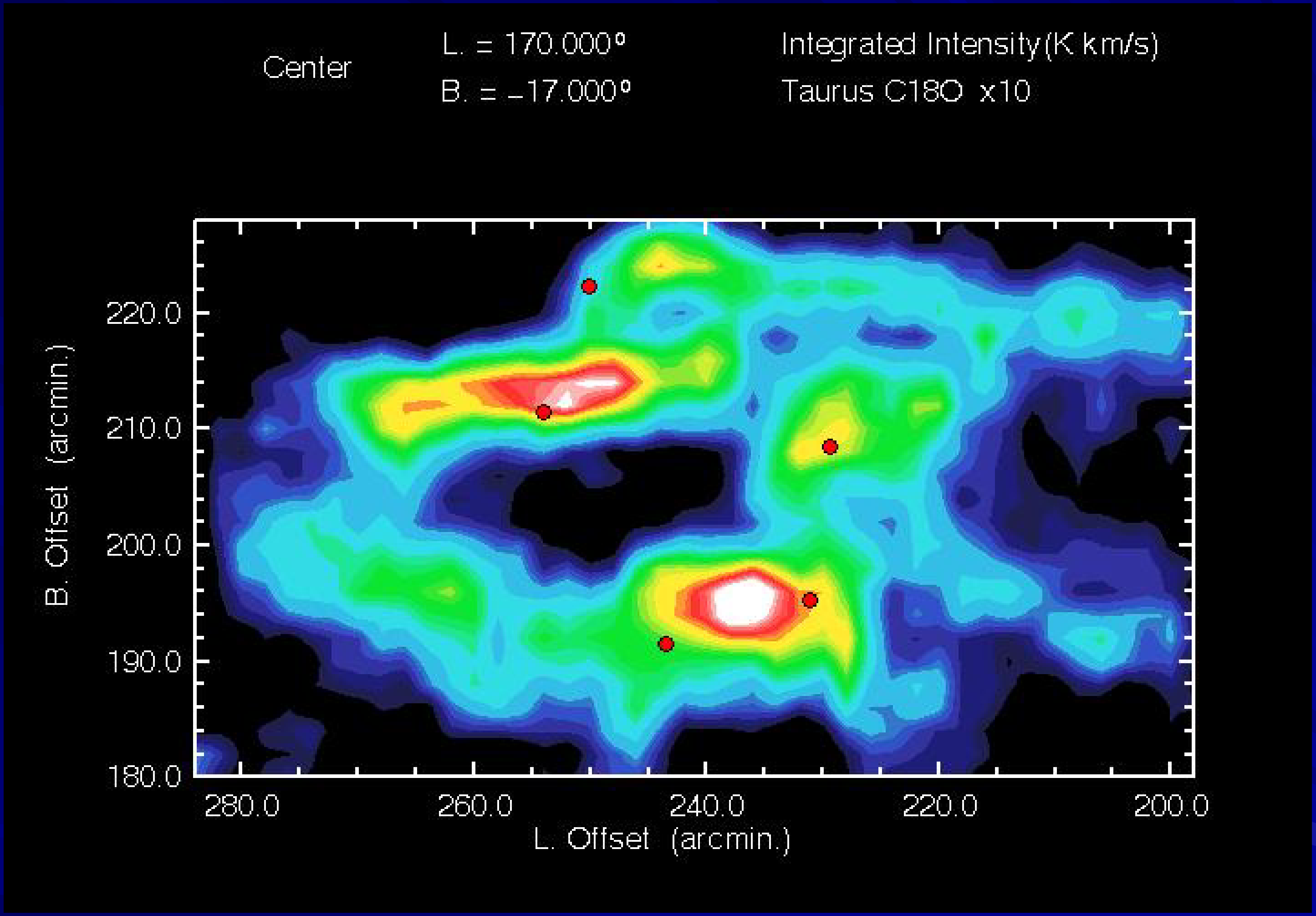

$C^{18}O$ integrated intensity map of HLC2 in Taurus molecular cloud. This shows the molecular cloud consists of many molecular cores.

Cores with/without Protostars

$H^{13}CO$

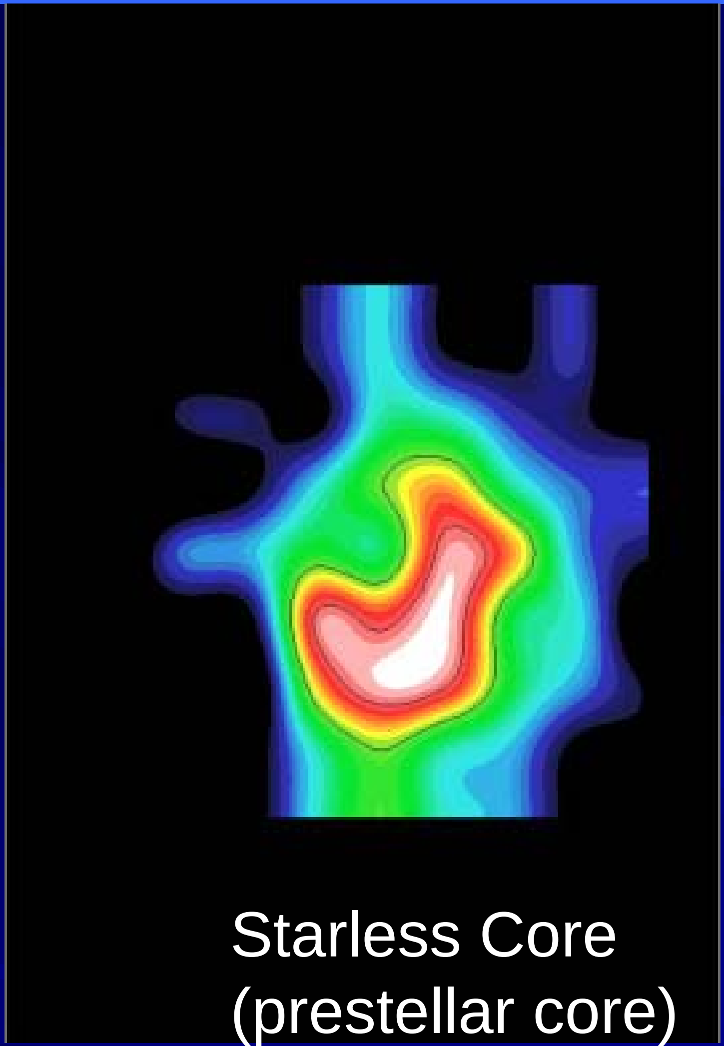

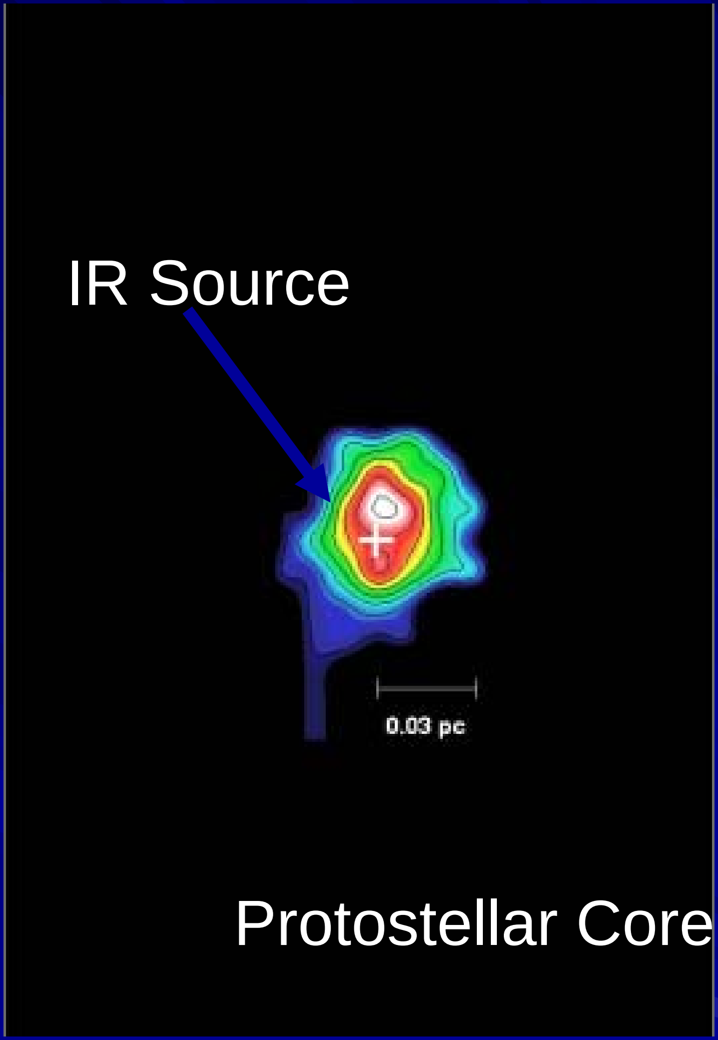

$H^{13}CO$ integrated intensity map of prestellar (left) and protostellar (right) cores in Taurus molecular cloud observed by Nobayama 45m radio telescope

Star Formation of ~$M_{\odot}$ stars

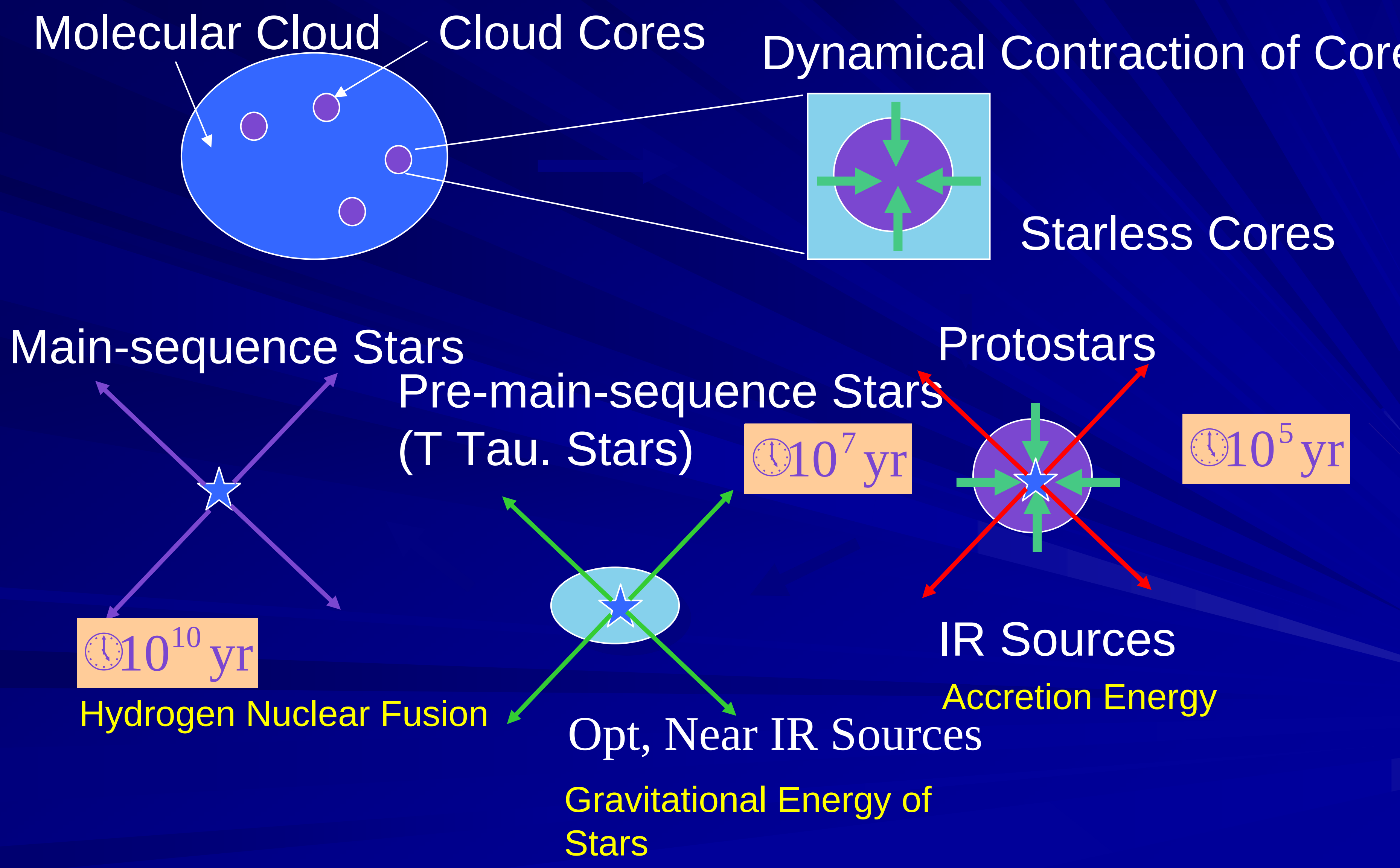

Spherical Collapse

Gas $(\mathbf{B}=0,\ \Omega=0)$ contracting under the self-gravity

Larson (1969)

- isothermal $\gamma = 1$ $\rho < \rho_A = 10^{-13}$ g cm^{-3}
  - ✓run-away collapse
  - ✓first collapse
- adiabatic $\gamma = 7/5$ $\rho_A < \rho < \rho_B = 5.6\ 10^{-8}$ g cm^{-3}
  - ✓first core
  - ✓outflow
  - ✓fragmentation
- H_2 dissociation $\gamma = 1.1$ $\rho_B < \rho < \rho_C = 2.0\ 10^{-3}$ g cm^{-3}
  - ✓second collapse

Temp-density relation of IS gas. (Tohline 1982)

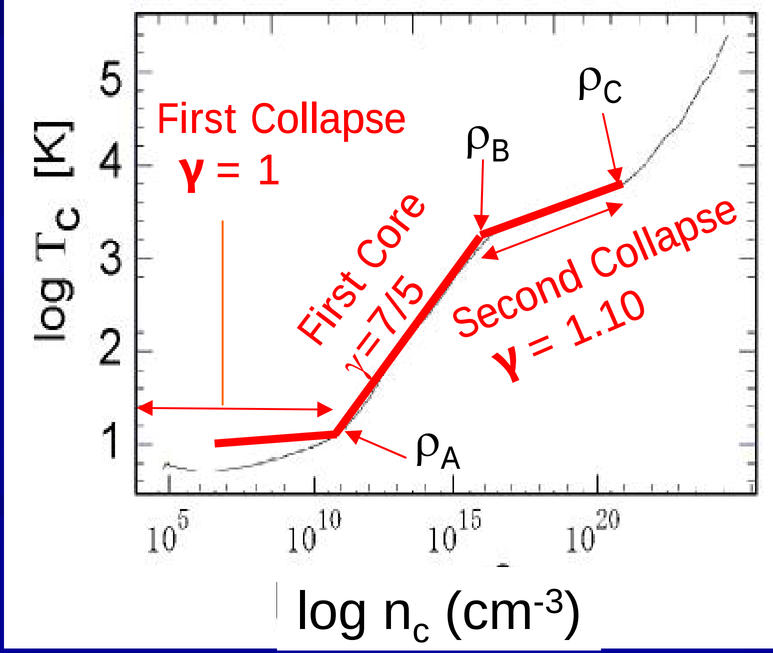

cf. Masunaga & Inutsuka (2000)

Runaway Collapse

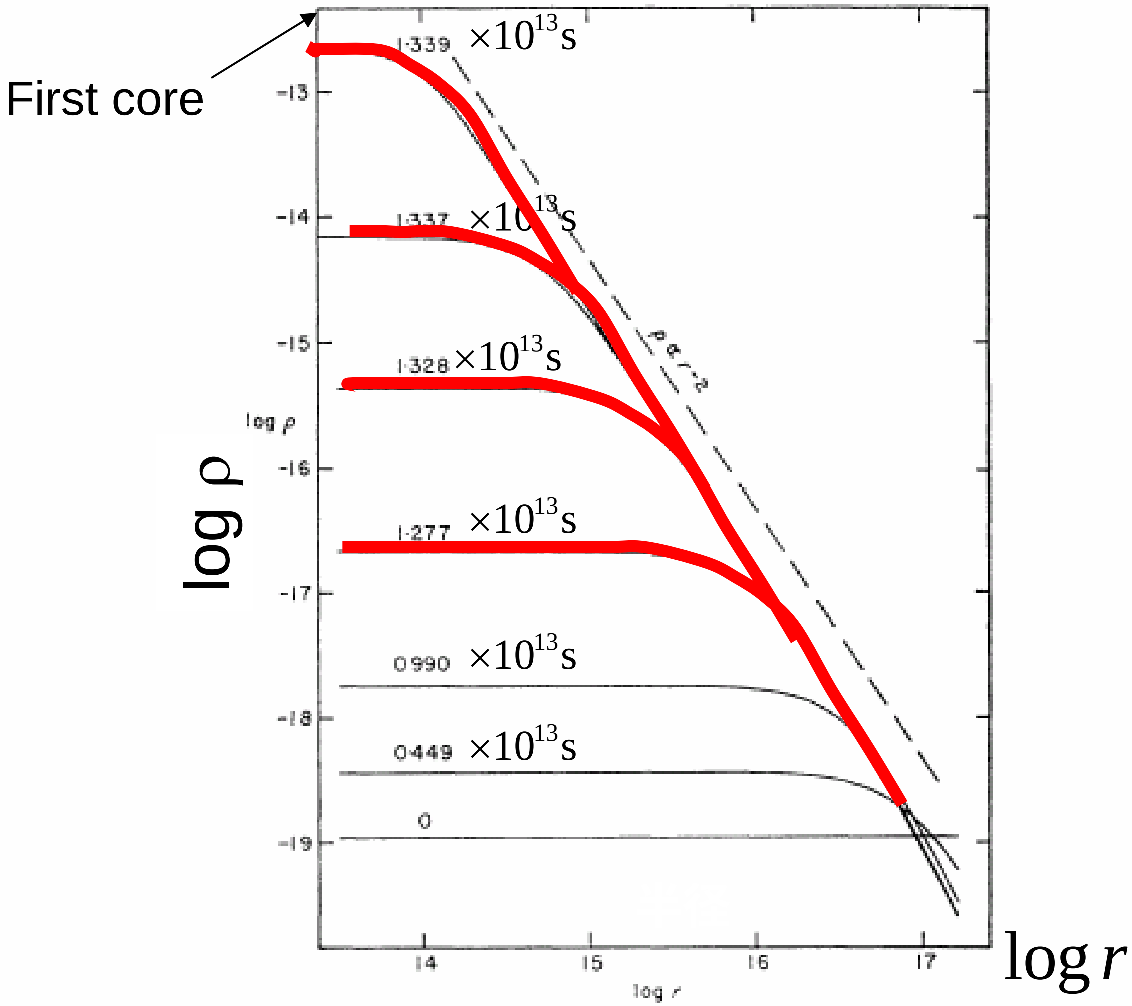

FIG. 1. *The variation with time of the density distribution in the collapsing cloud (CGS units). The curves are labelled with the times in units of* 10^{13} *s since the beginning of the collapse. Note that the density distribution closely approaches the form* $\rho \propto r^{-2}$.

Isothermal spherical collapse shows:

(1) Convergence to a power-law structure

$$\rho(r) \propto r^{-2}$$

(2) Increase of central density in a finite time.

(3) Only a central part contracts.

This is called "runaway collapse."

Larson 1969, MNRAS, 145,271

$\mathbf{B}, \mathbf{\Omega} \neq 0$

How about a Rotating Magnetized Cloud?

1. In case with B and Ω, a runaway contracting disk is made. As a consequence,
   (a) A flat first core is born.
   (b) Outflow is driven by a twisted B-field and a rotating disk.
   (c) B-field transfers the angular momentum from the contracting disk to the envelope.
3. Star formation process is controlled by the rotation speed of the first core.
   (a) A slow rotator evolves similarly to the B=Ω=0 cloud.
   (b) A first core with Ω in a finite range,
   (c) A fast rotator fragments, which leads to binary formation.

Initial Condition

Numerical Method

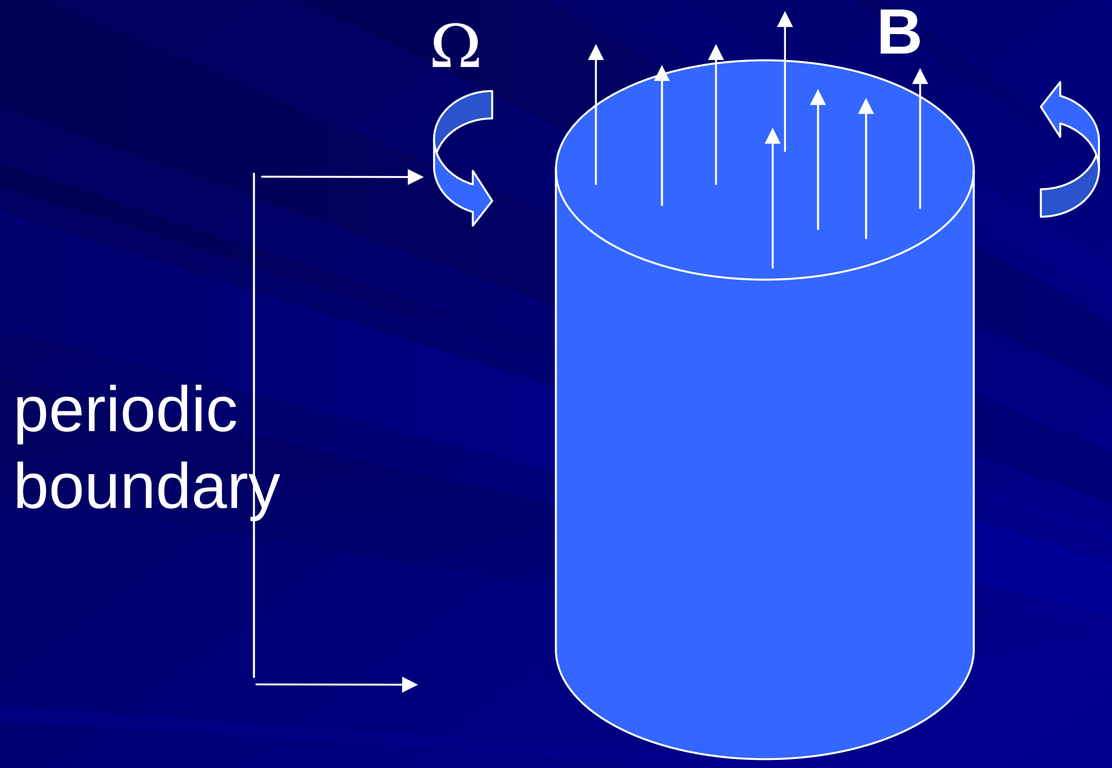

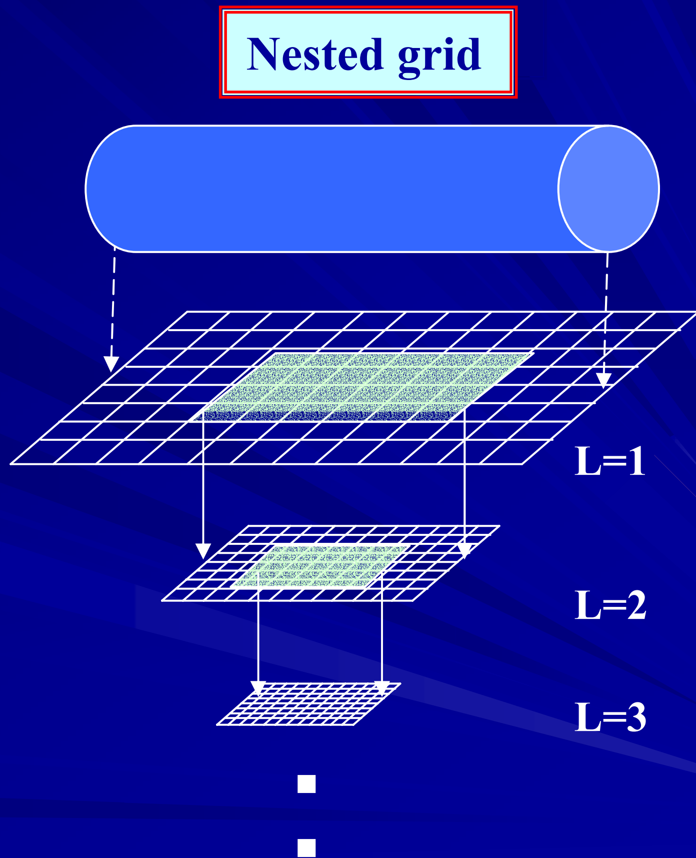

axisymmetric ρ perturbation

nonaxisymmetric ρ perturbation

The coarsest grid

Nested 4-times finer grid

Ω ρ Ω ρ

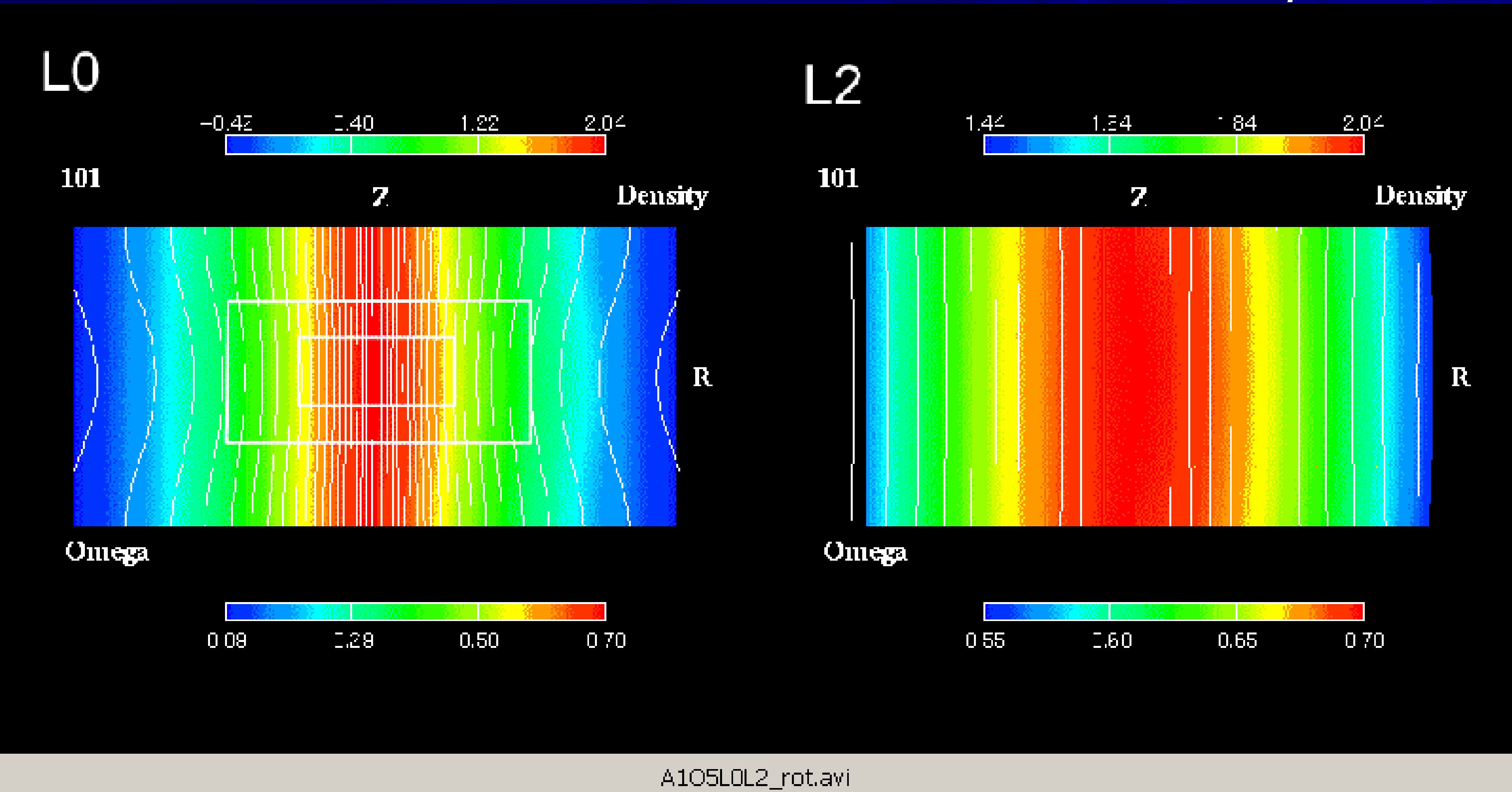

Nested 2^8-times finer grid

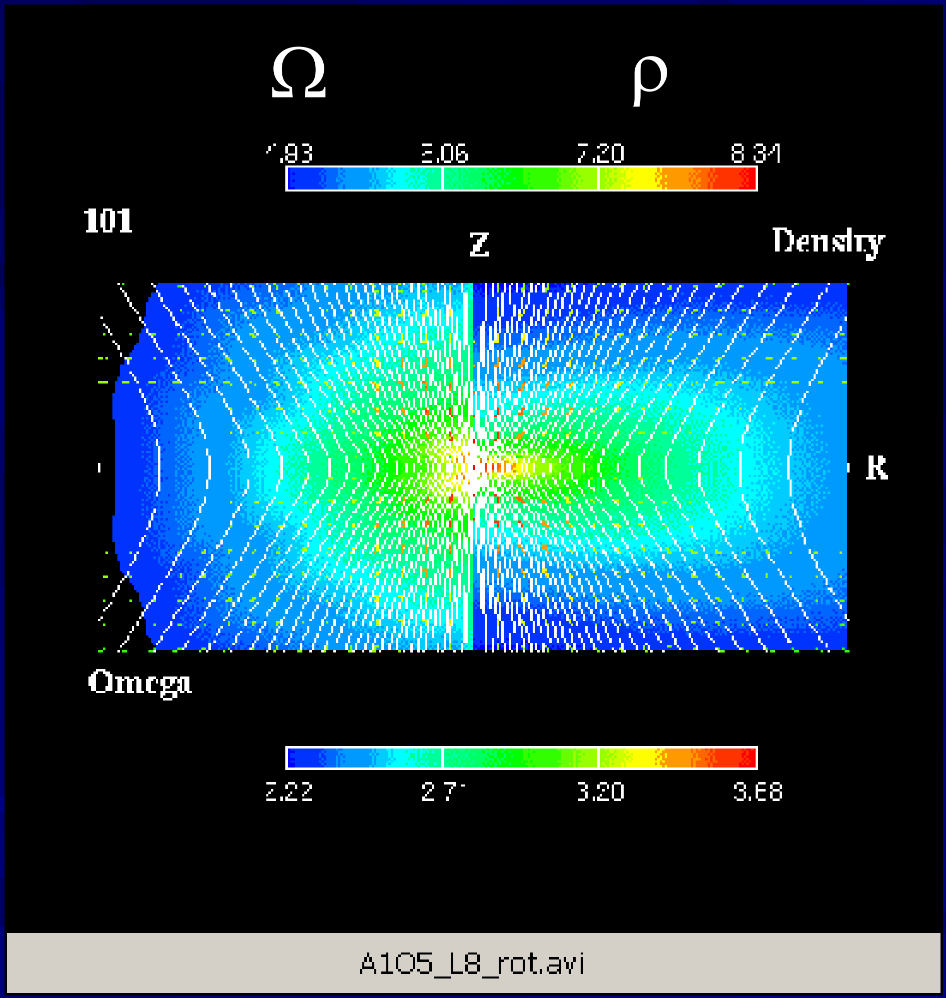

(1)Just after the central density exceeds ρ_A (first core formation), outflow begins to blow.

(2) In this case, gas is accelerated by the magnetocentrifugal wind mechanism.

(3) 10% of gas in mass is ejected with almost all the angular momentum.

ビデオ クリップ

Angular Momentum Redistribution in Dynamical Collapse

- In outflows driven by magnetic fields:
  - The angular momentum is transferred effectively from the disk to the outflow.
  - If 10 % of inflowing mass is outflowed with having 99.9% of angular momentum, j_* would be reduced to 10^{-3} j_{cl}.

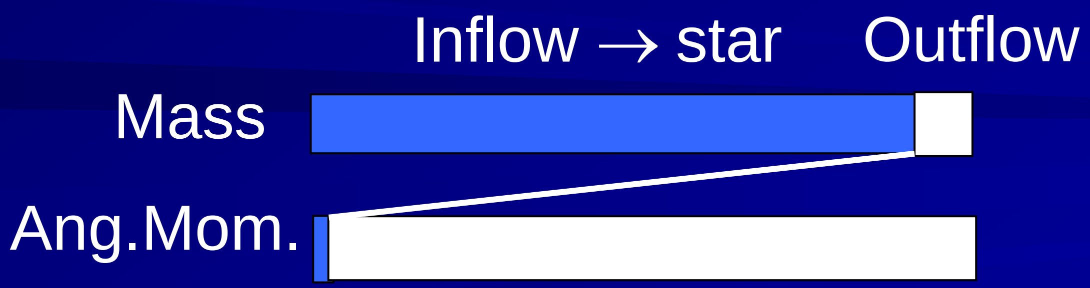

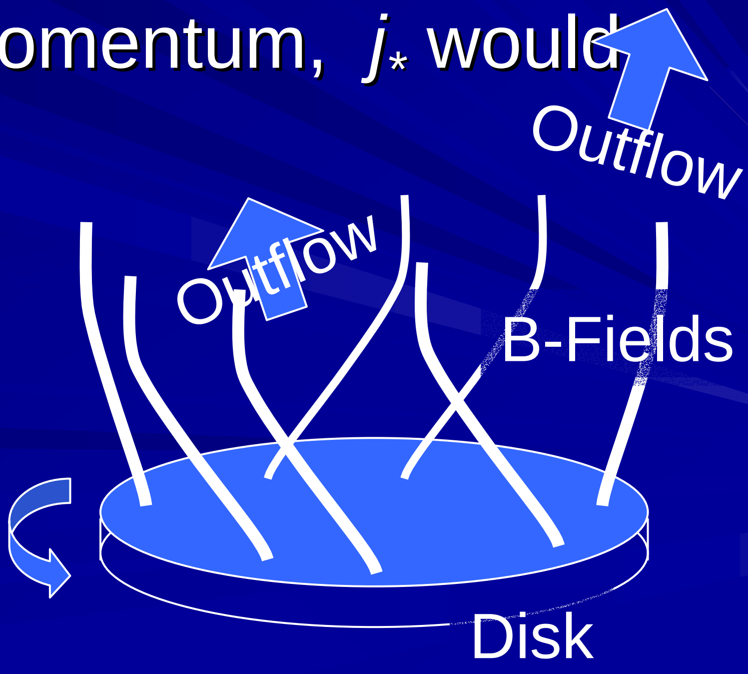

Angular Momentum Problem

- Specific Angular Momentum of a New-born Star

$$j_* \approx 6 \times 10^{16} \left(\frac{R_*}{2R_\odot}\right)^2 \left(\frac{P}{10\mathrm{day}}\right)^{-1} \mathrm{cm^2 s^{-1}}$$

- Orbital Angular Momentum of a Binary System

$$j_{\rm bin} \approx 4 \times 10^{19} \left(\frac{R_{\rm bin}}{100\mathrm{AU}}\right)^{1/2} \left(\frac{M}{M_\odot}\right)^{1/2} \mathrm{cm^2 s^{-1}}$$

- Specific Angular Momentum of a Parent Cloud Core

$$j_{\rm cl} \approx 5 \times 10^{21} \left(\frac{R}{0.1\mathrm{pc}}\right)^2 \left(\frac{\Omega}{4\mathrm{km s^{-1} pc^{-1}}}\right) \mathrm{cm^2 s^{-1}}$$

- Centrifugal Radius

$$R_c = \frac{j^2}{GM} \approx 0.06\mathrm{pc} \left(\frac{j}{5 \times 10^{21} \mathrm{cm^2 s^{-1}}}\right)^2 \left(\frac{M}{M_\odot}\right)^{-1}$$

$j_{\rm cl} \gg j_*$

$j_{\rm cl} >> j_{\rm bin}$

$R_c \gg R_*$

$R_c >> R_{\rm bin}$

Tomisaka 2000 ApJL **528** L41--L44

Angular Momentum Distribution

(1) Mass measured from the center

$$M(\rho < \rho_1) = \int_{\rho < \rho_1} \rho \, dV$$

(2) Angular momentum in $M(\rho < \rho_1)$

$$L(\rho < \rho_1) = \int_{\rho < \rho_1} \rho r v_\phi \, dV$$

(3) Specific Angular momentum distribution

$$j(\Delta M) = \frac{L(\rho < \rho_1)}{M(\rho < \rho_1)}$$

Angular Momentum Transfer

Run-away Collapse

High-density region is formed by gases with small *j*.

Accretion Stage

Magnetic torque brings the angular momentum from the disk to the outflow.

Outflow brings the angular momentum.

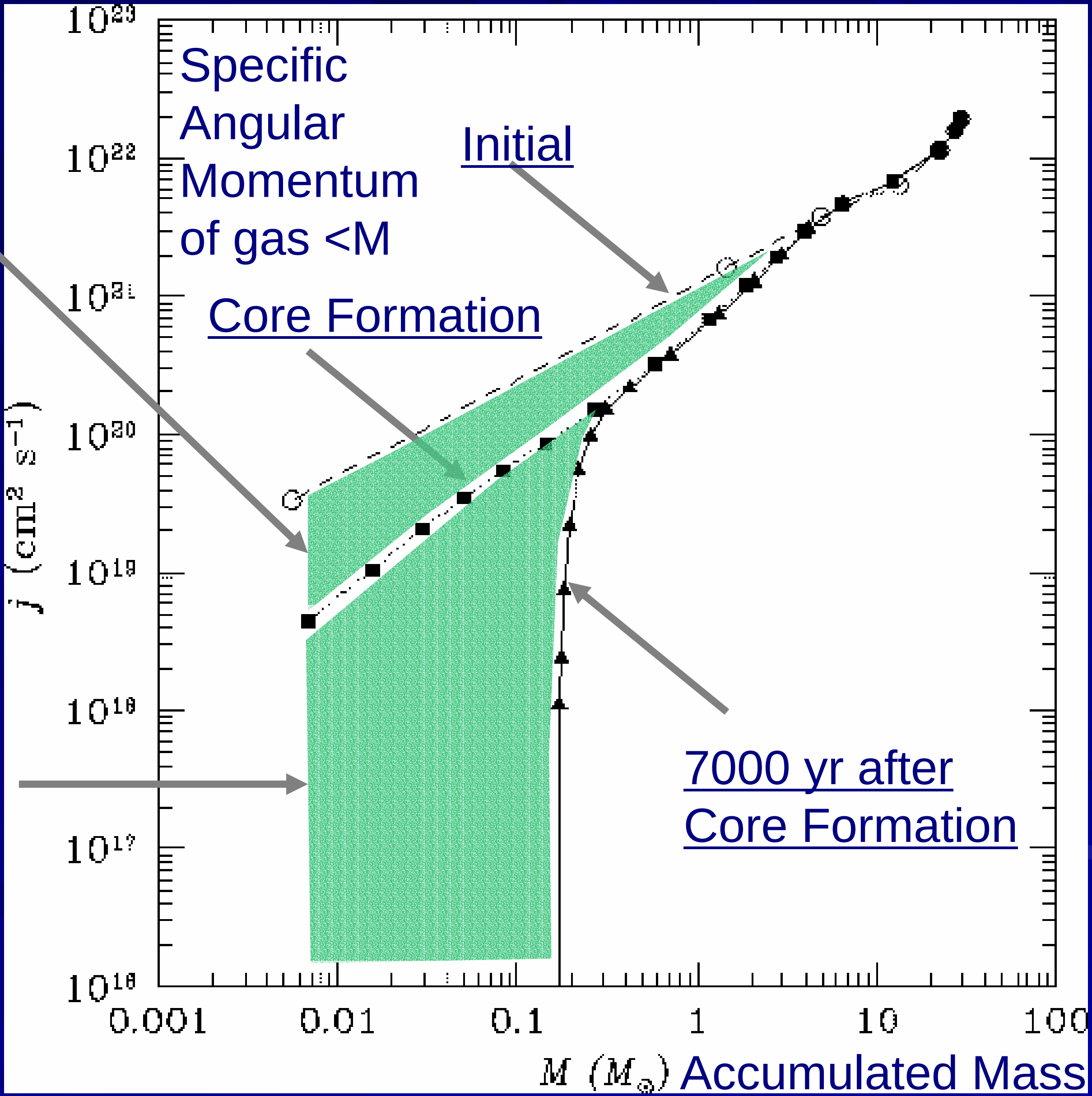

アウトフローの働き

角運動量と質量の分離

星･惑星系形成時の角運動量過剰問題の解決

Entrainment vs 2 outflows

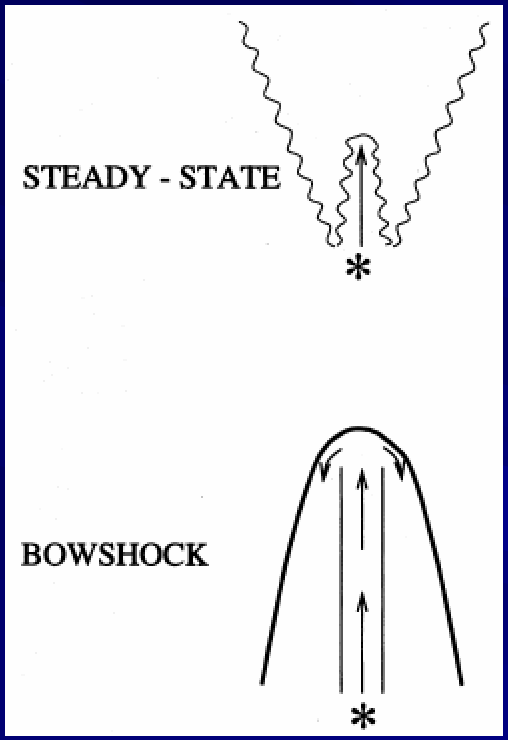

- 分子流の角運動量配分は質量配分に比例。
  - 角運動量問題を解決しない。

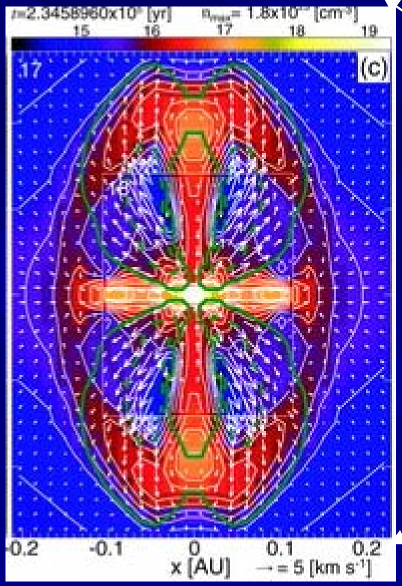

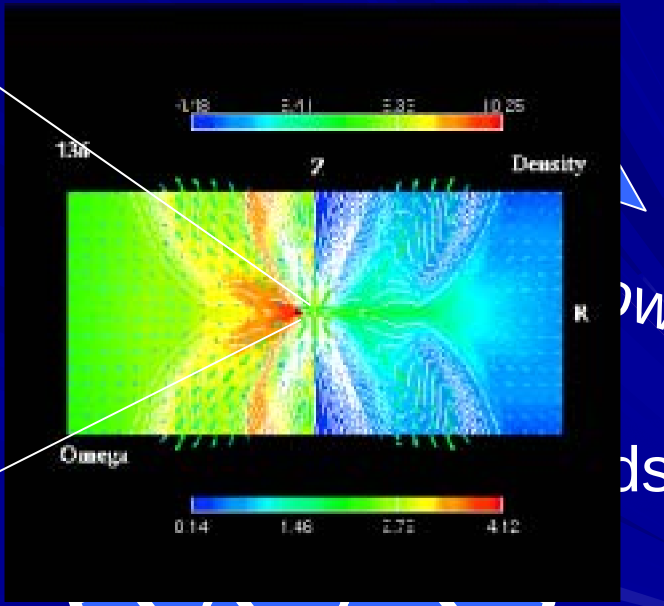

- 分子流の角運動量配分は質量配分より非常に多い。
  - 角運動量問題を解決する。

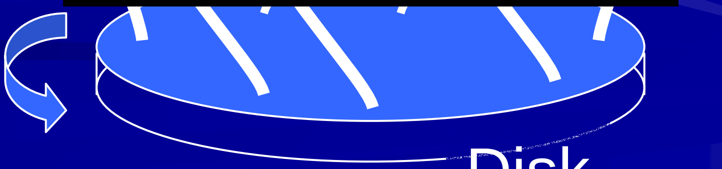

Molecular Outflow

L1551 IRS5

^{12}CO $J = 1 \rightarrow 0$

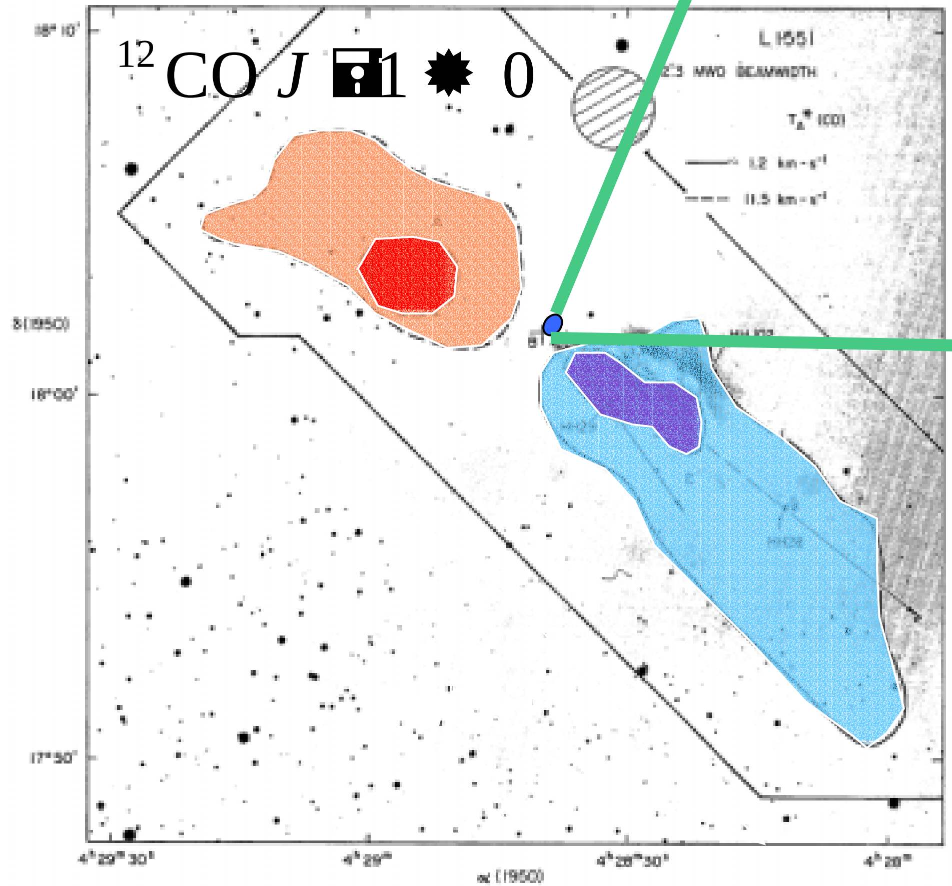

Snell, Loren, &Plambeck 1980

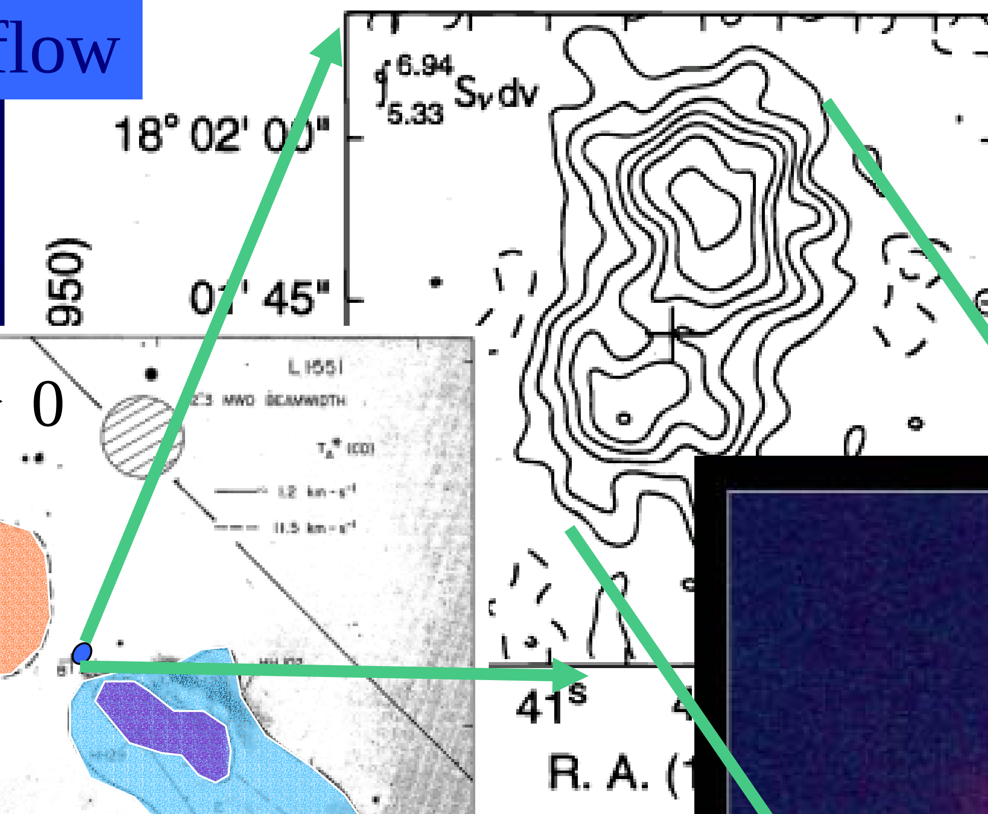

$H^{13}CO^+$

Saito, Kawabe, Kitamura&Sunada 1996

Optical Jets

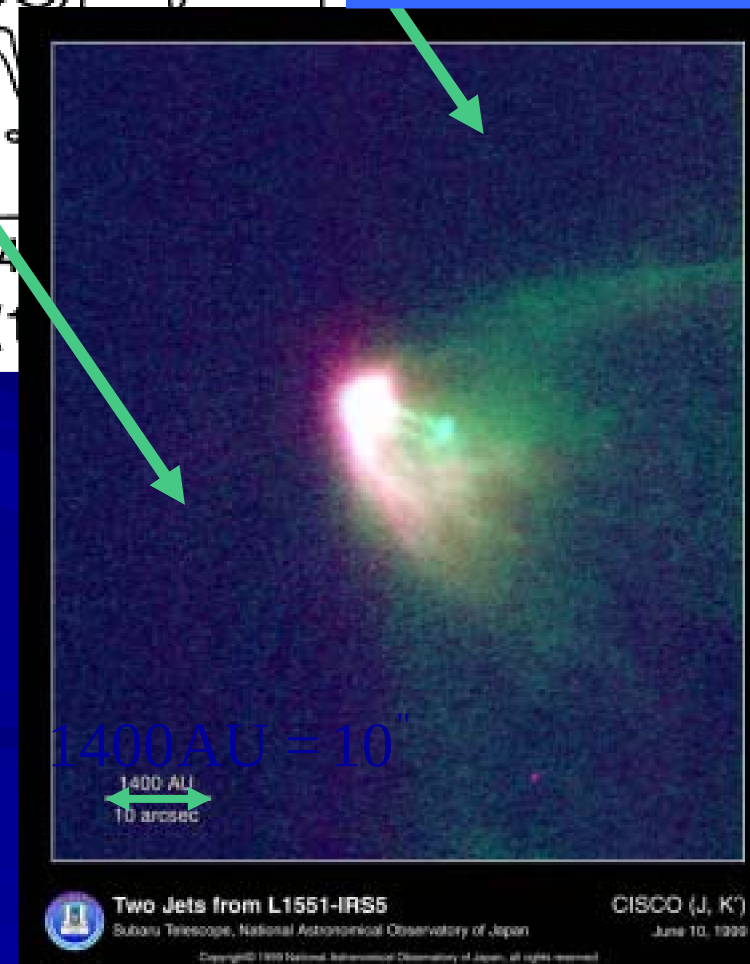

Binary: To understand Star Formation, study BINARY FORMATION.

Binary fraction is high.

TABLE 6. Multiplicity of T Taur stars in the complete samp

Sample	# Targets	# Companions in completeness region	bsf[b] (%)
Total	64	22	34±7
Oph–Sco	21	6	29±12
Tau–Aur	43	16	37±9
WTTS	22	8	36±13
CTTS	42	14	33±9
$\mathcal{M} < 1\mathcal{M}_\odot$	32	13	41±11
$\mathcal{M} > 1\mathcal{M}_\odot$	32	9	28±9

[a]The complete sample, discussed in Sec. 5.1, includes all observations sensitive to the "completeness region," i.e., that revealed all companion stars within the projected linear separation range 16 to 252 AU and within the magnitude difference range 0 to 2.0 mag.
[b]The restricted binary star frequency (bsf) incorporates only companion stars within the completeness region, and is therefore a lower limit to the true binary star frequency in the separation range 16 to 252 AU. Nonetheless, it is useful for comparisons of various groups of T Tauri stars, which are discussed in the sections listed in Column 5.

ΔK<2mag

if completely surveyed, bsd ~60%

Ghez et al 1993

Period distribution of nearby binaries

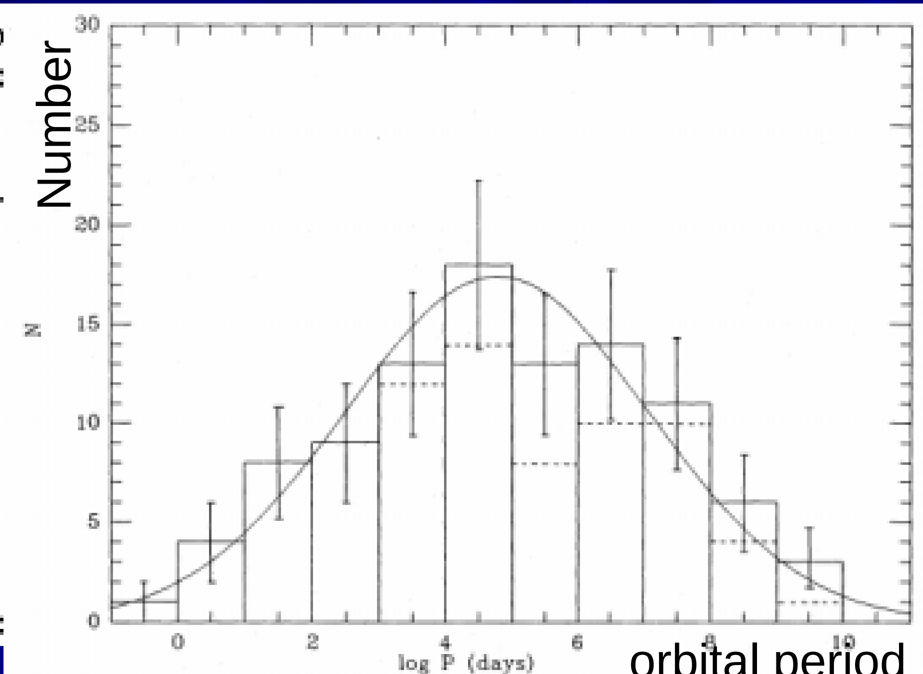

Fig. 7. Period distribution in the complete nearby G-dwarf sample, without (dashed line) and with (continuous line) correction for detection biases. A Gaussian-like curve is represented whose parameters are given in the text

Gaussian around ~180yr

Duquennoy & Mayor 2001

Binary Fraction

This suggests binary/multiple systems are formed in early phase.

(1) may depend on the mass of the stars

- Herbig/AeBe 68±11% (SSB) (Baines et al. 06)
- similar to T Tau

(2) may be deferent between PMS and MS.

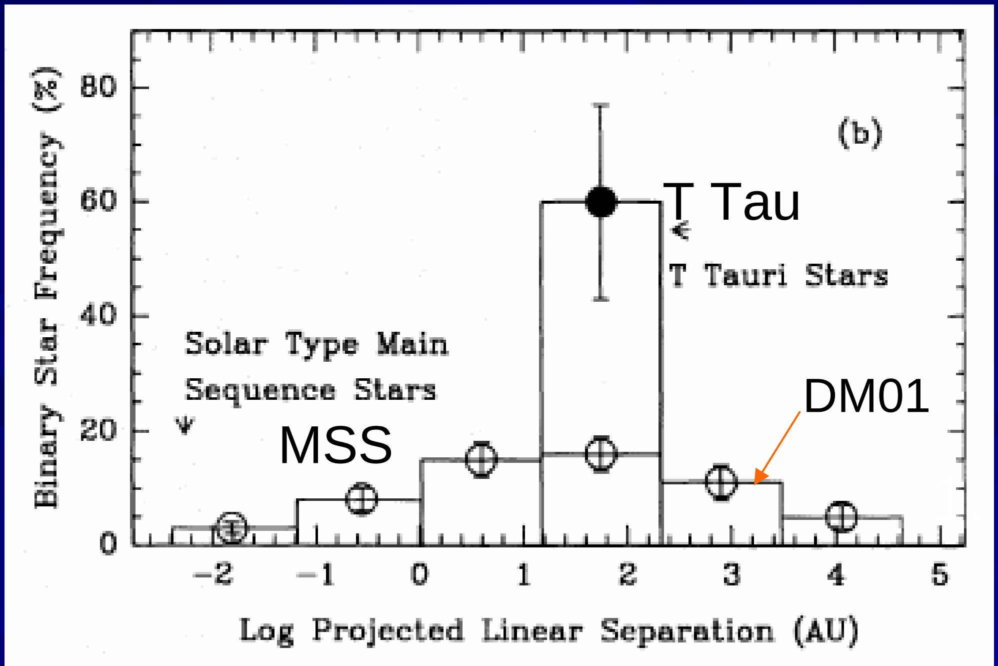

Ghez et al 1993

(3) may depend on the local stellar density

Liu et al. 2003

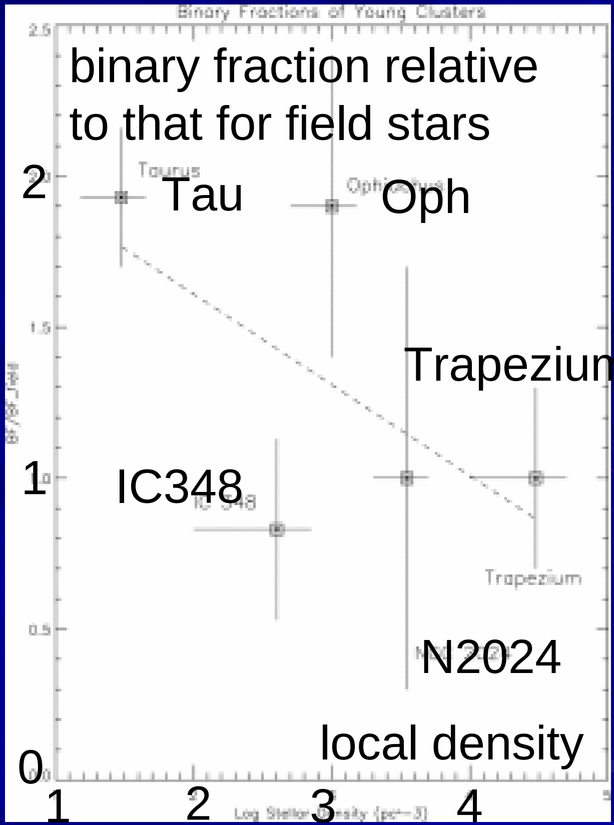

Binary fraction is a decreasing function of local stellar density

3D MHD Simulation of Rotating Magnetized Cloud Collapse

Machida, Tomisaka, Matsumoto 04
Machida, M.,H., Tomisaka, 05
Machida, M. Tomisaka, H. 05
Machida, M.,H., Tomisaka, 06

Model and Numerical Method

- Assume barotropic eq. state.
  - mimicing the result of 1D RHD (eg. Masunaga, Inutsuka 2000).

$$p = c_s^2 \rho + c_s^2 \rho_{crit} \left(\rho / \rho_{crit} \right)^{7/5}$$

$$n_{crit} = 5 \times 10^{10}\,\mathrm{cm}^{-3}$$

$$p \approx \begin{cases} c_s^2 \rho \ \mathrm{K} & (\rho \le \rho_{crit}) \\ K \rho^{7/5} \mathrm{K} & (\rho > \rho_{crit}) \end{cases}$$

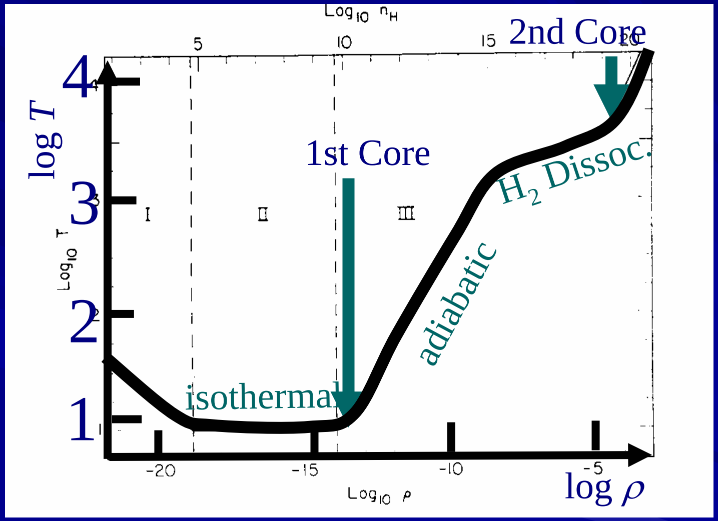

Temp-density relation of IS gas.
(Tohline 1982)

- Ideal MHD

$$\begin{cases} \dfrac{\partial \rho}{\partial t} + \nabla \cdot (\rho \mathbf{v}) = 0, \\ \rho \left(\dfrac{\partial \mathbf{v}}{\partial t} + \mathbf{v} \cdot \nabla \mathbf{v} \right) = -\nabla p - \rho \nabla \phi, \\ \dfrac{\partial \mathbf{B}}{\partial t} + \nabla \times (\mathbf{v} \times \mathbf{B}) = 0, \\ \Delta \phi = 4\pi G \rho \end{cases}$$

Numerical Method (cont.)

- Non-homologous Collapse
  - Dynamic ranges of size and density scales are huge.

$$\rho_{\mathrm{ISM}} : 10^{2}\,\mathrm{cm}^{-3} \qquad \rho_{\mathrm{2ND\ CORE}} : 10^{17}\,\mathrm{cm}^{-3}$$
$$L_{\mathrm{ISM}} : 0.1\mathrm{pc} \qquad L_{\mathrm{2ND\ CORE}} : 10^{11}\,\mathrm{cm}$$

- "Nested Grid" Technique
  - Coarser grid: covers global structure
  - Finer grid: small-scale structure near the center.
    - # of cells：128(x)✕128(y)✕32(z)✕17 (level)
    - equivalent to simulations with〜1.5×10^{20} grids at the center.

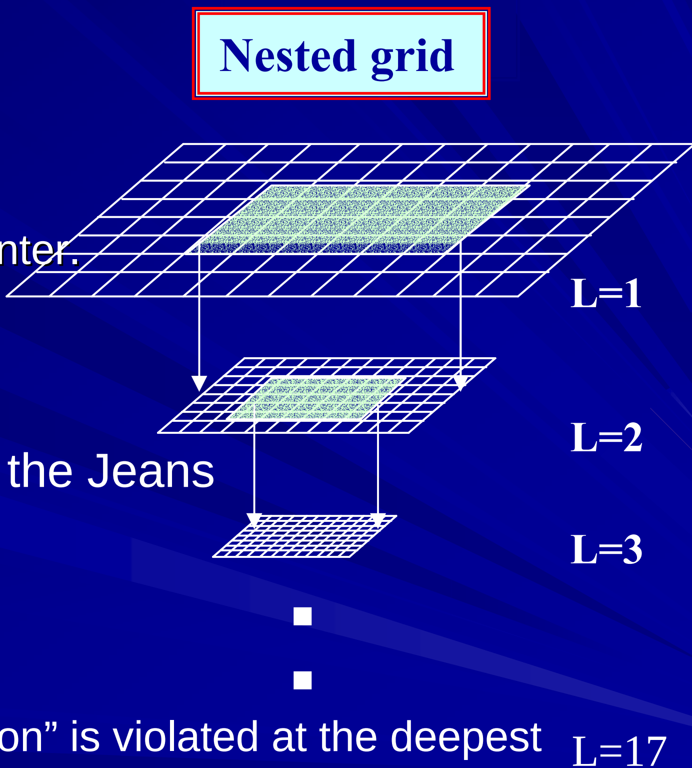

- New Finer Grid is Generated to Guarantee the Jeans Condition (Truelove et al. 1997)
  - To achieve physically correct answer:

$$\Delta x < \lambda_{\mathrm{J}} / 4 = [(4\pi G\rho)^{1/2} / c_s]/4$$

  - Simulations continues till the "Jeans Condition" is violated at the deepest level of grid (17th Level).

Initial Condition

- An isothermal cylindrical cloud
  - in hydrostatic balance (Stodolkiewicz
    - $\mathbf{\Omega} \,//\, \mathbf{B} \,//\, \mathrm{F}$
    - $B \propto \rho^{1/2}$;

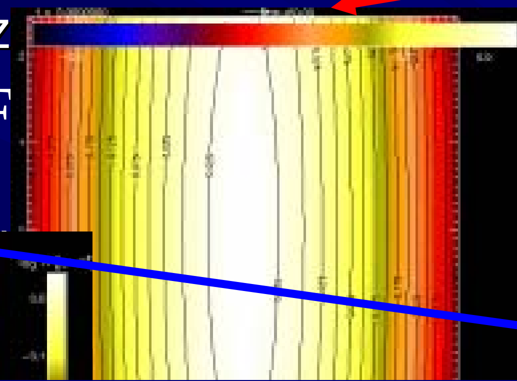

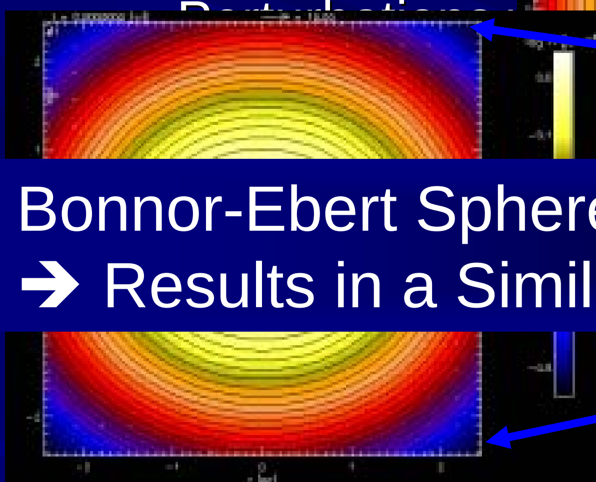

well as

ode

Bonnor-Ebert Sphere with Rigid-body Rotation & Uniform B-Field
➔ Results in a Similar Result.

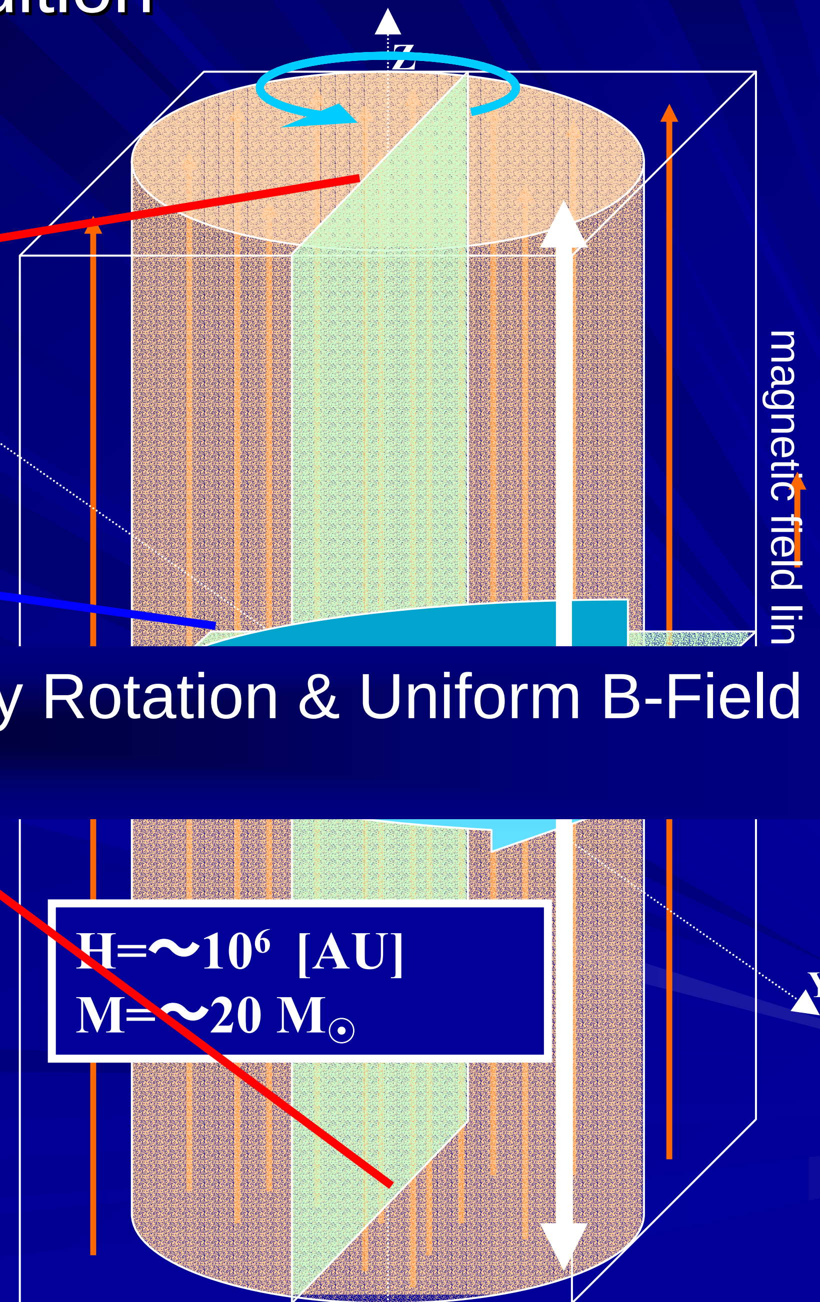

- Parameters:
  - B-field strength and angular rotation speed: $A\phi$,

$$\alpha = \frac{B_{0c}^2 / 4\pi}{c_s^2 \rho_{0c}} \qquad \omega = \Omega\left(4\pi G \rho_{0c}\right)^{-1/2}$$

3.Results

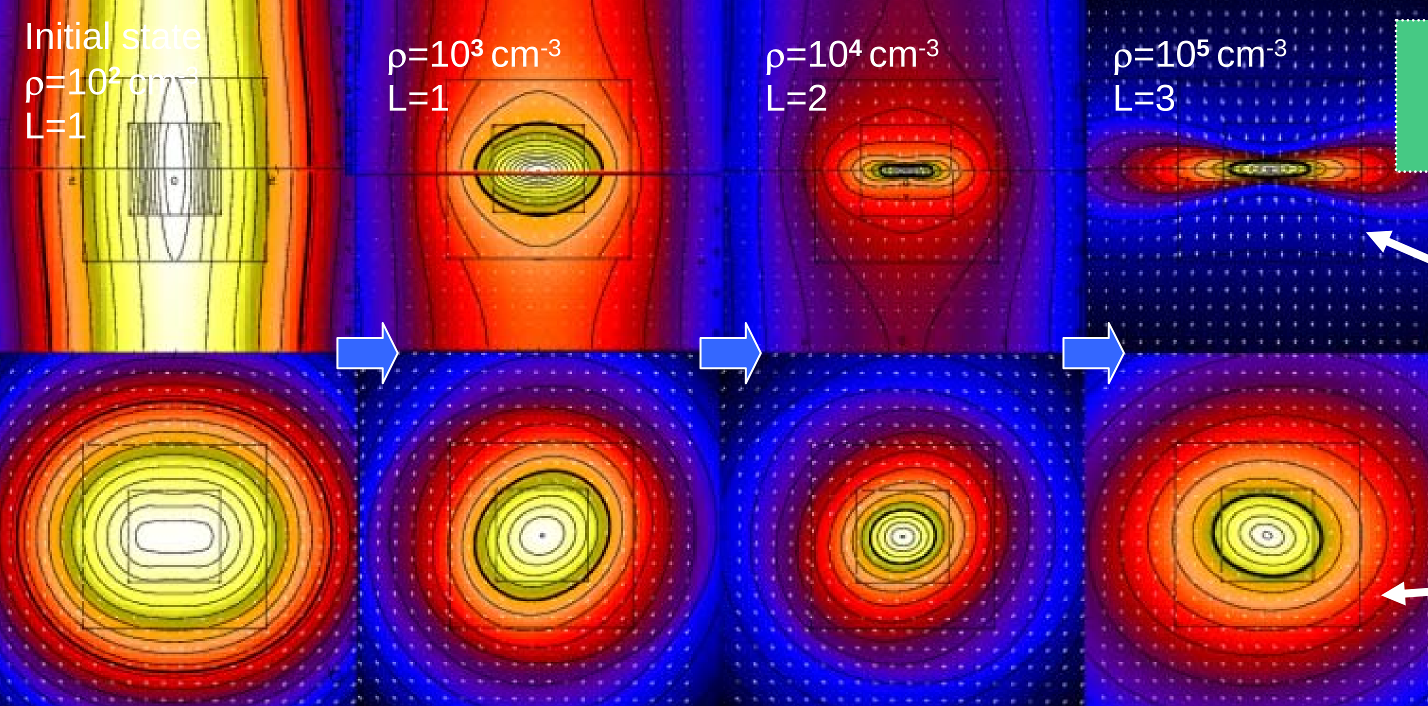

Side view

x=0 plane

Pole-on view
z=0 plane

$(A_{m2}, \alpha, \omega)=(0.2, 1, 0.5)$

Model with strong magnetic field and high rotation speed

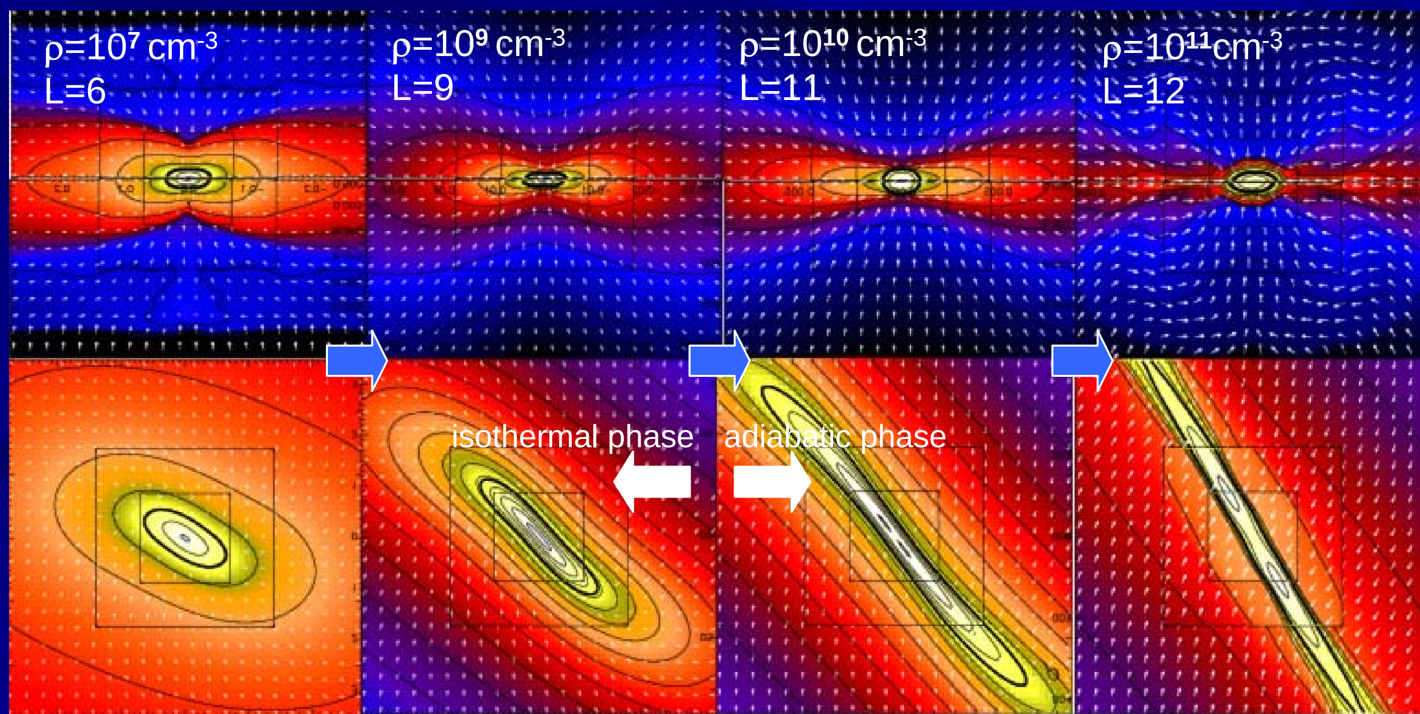

Only after the sufficiently thin disk is formed, the non-axisymmetric perturbation can grow

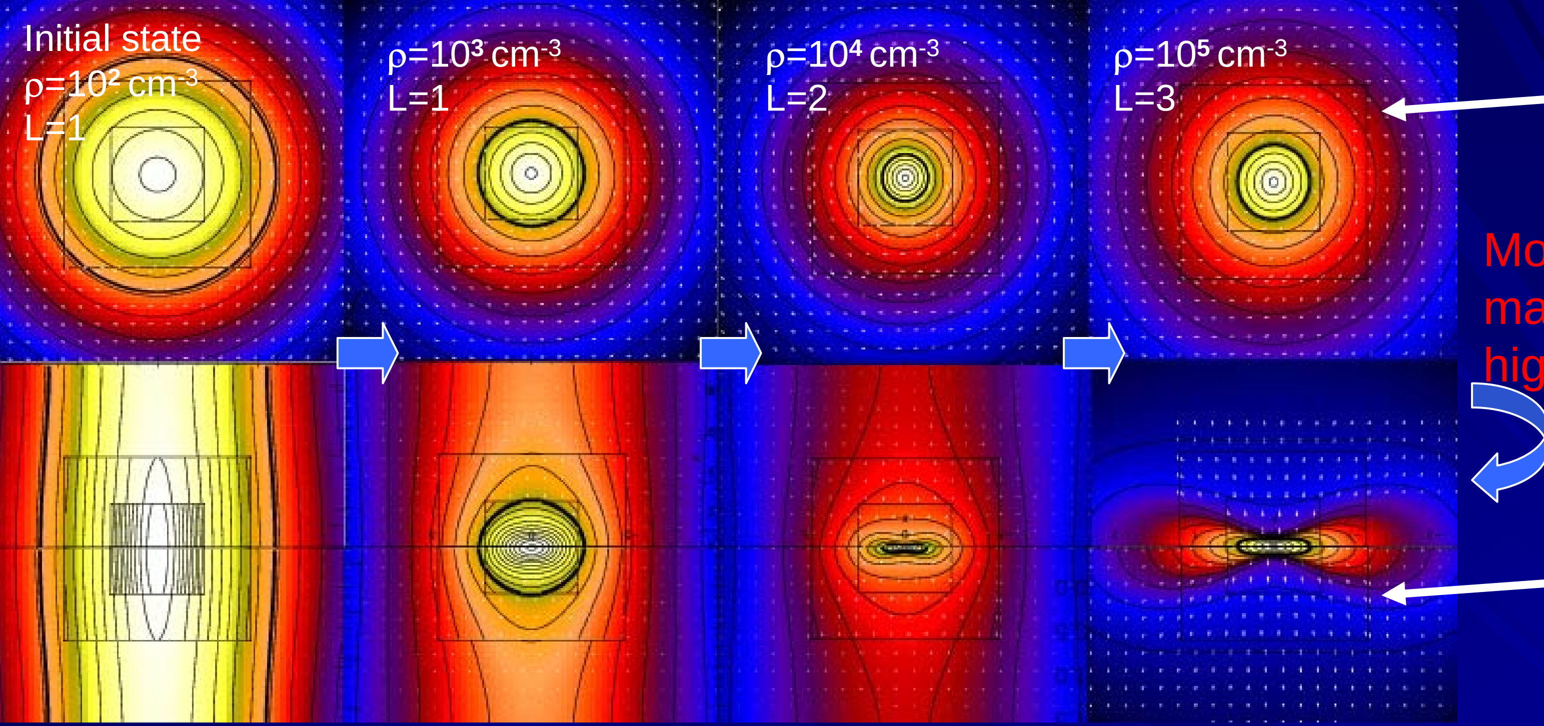

Pole-on view

z=0 plane

Model with weak magnetic field and high rotation speed

Side view

x=0 plane

Typical Model

$(A_{m2}, \alpha, \omega)=(0.01, 0.01, 0.5)$

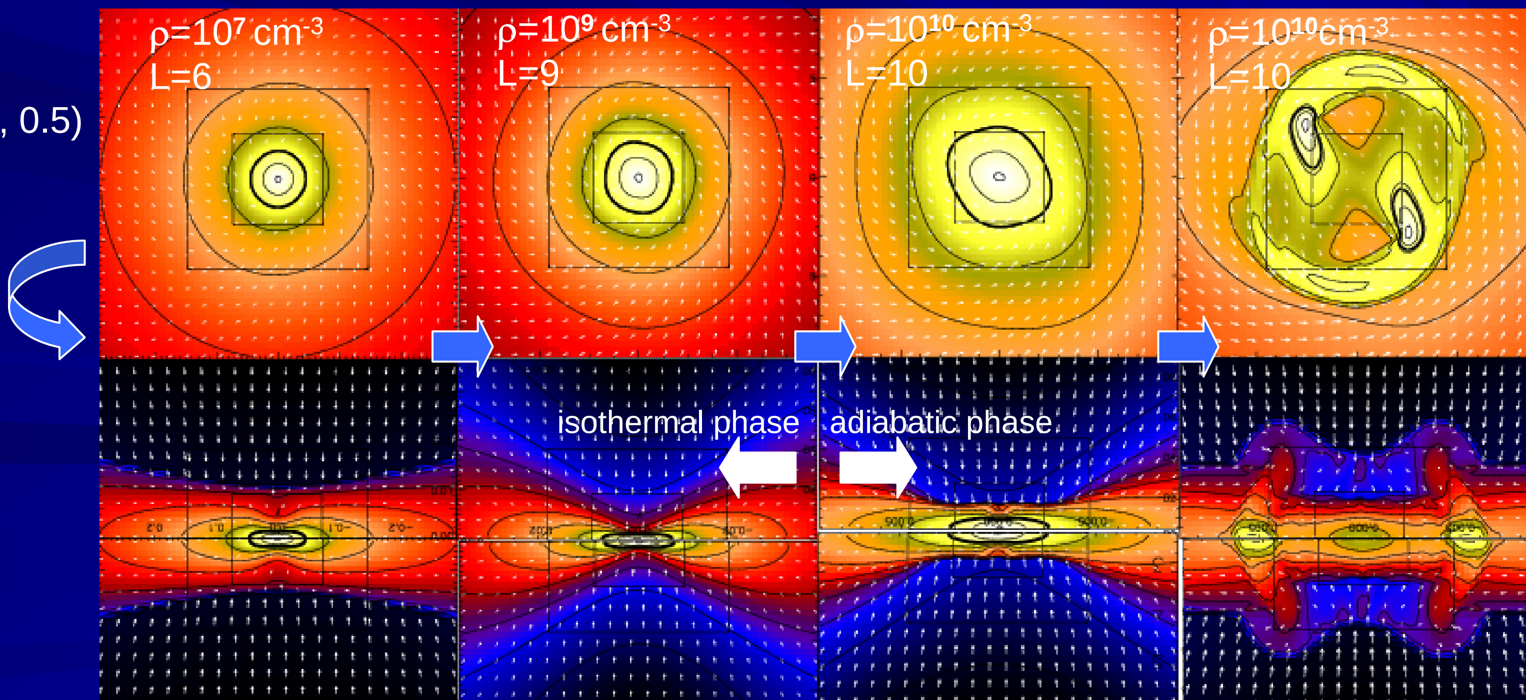

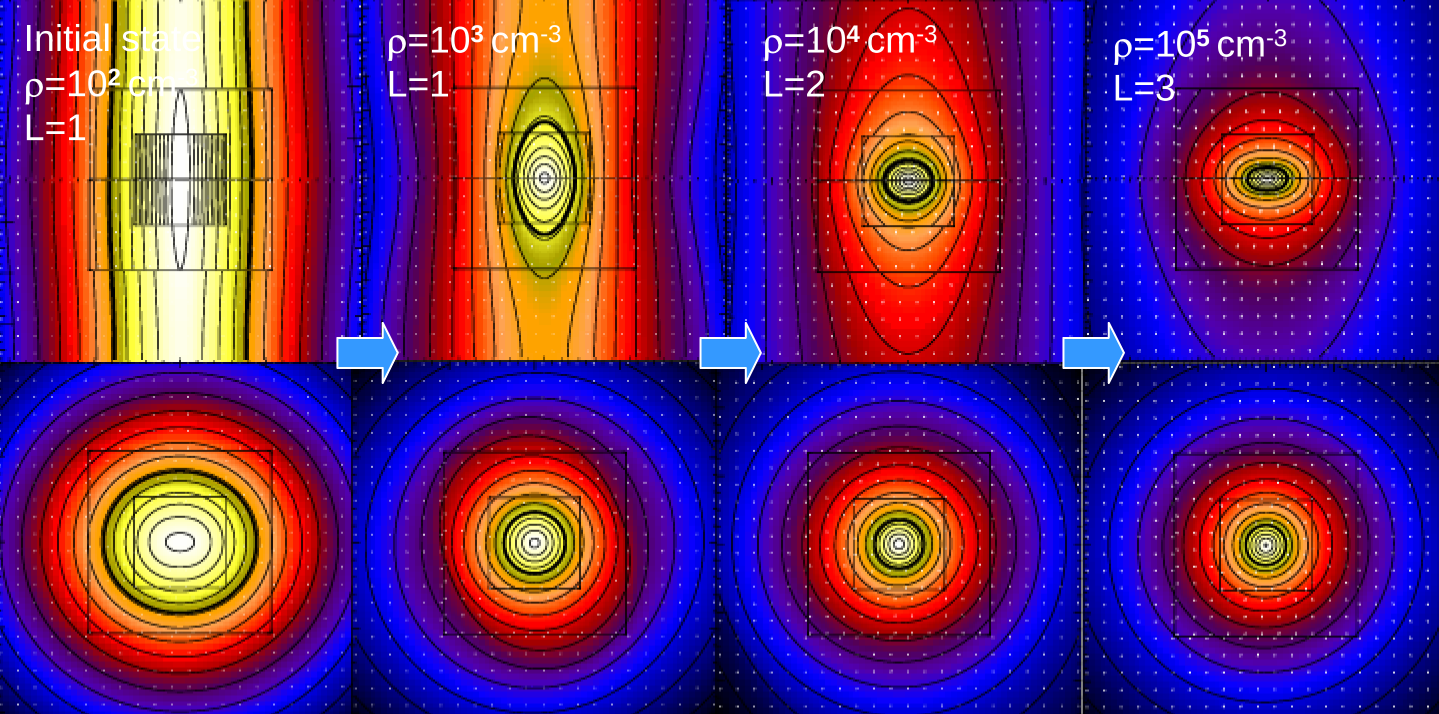

This corresponds to strong B-field & slow rotation.

Disk -->
Spherical core

Core Model

(A_{m2}, α, ω)=(0.01, 1, 0.1)

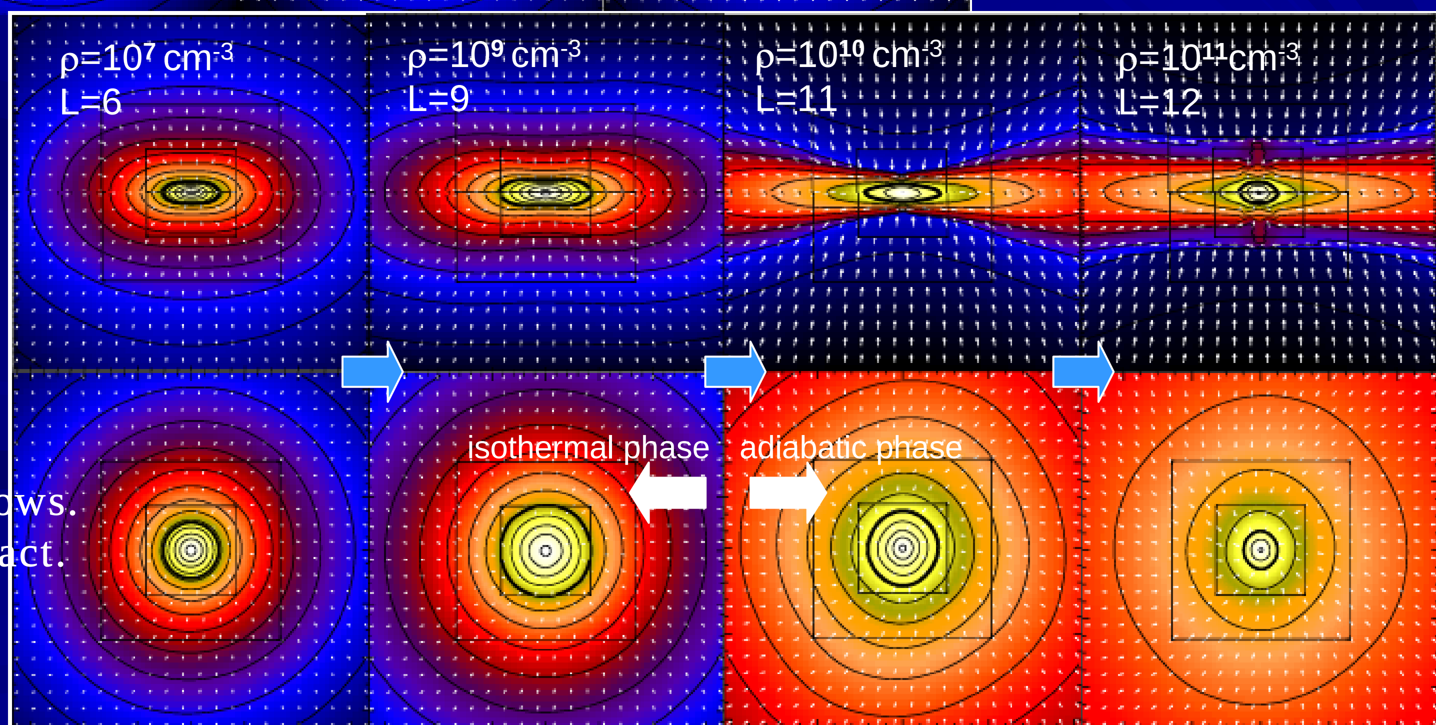

In this model, the non-axisymmetry hardly grows. Core continues to contract.

Bar Fragmentation

$A = 0.2,\ \alpha = 1,\ \omega = 0.5$

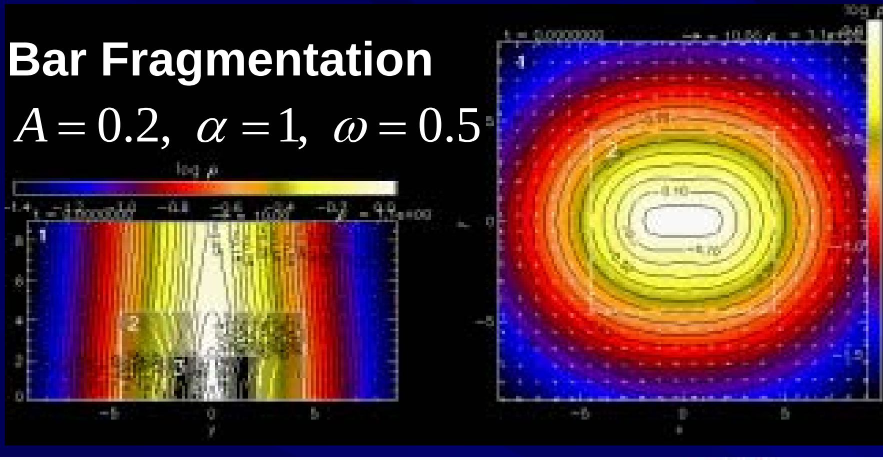

Ring Fragmentation

$A = 0.01,\ \alpha = 0.01,\ \omega = 0.5$

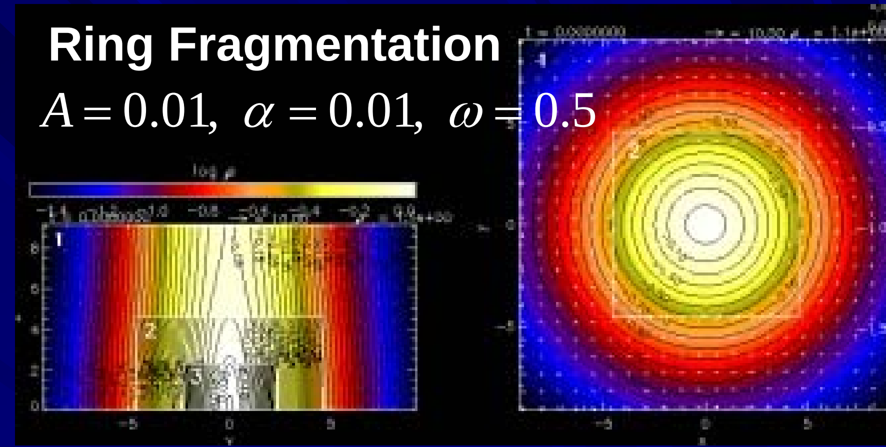

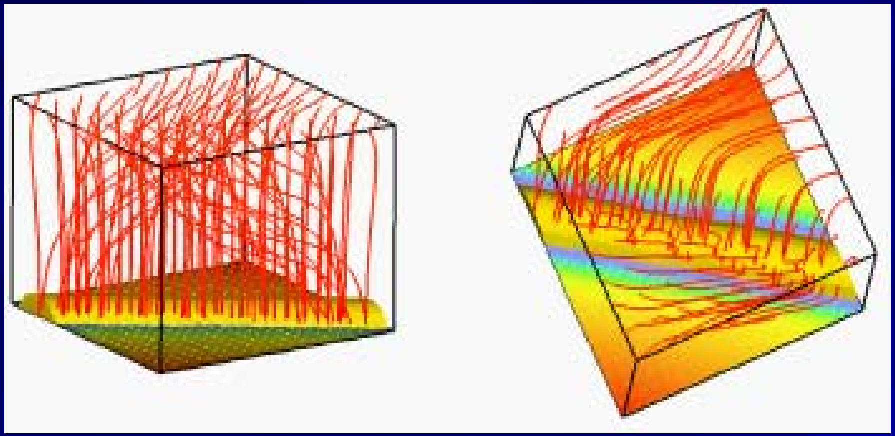

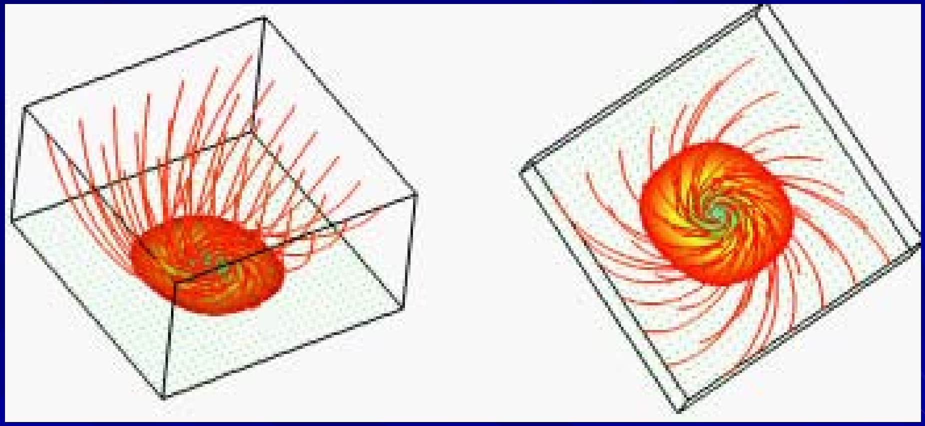

Non-Fragmentation

$A = 0.01,\ \alpha = 1,\ \omega = 0.1$

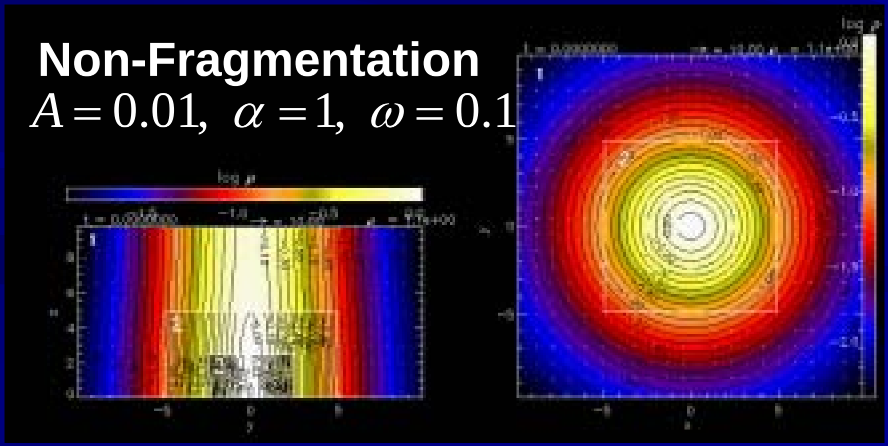

Non-Fragmentation

$A = 0.01,\ \alpha = 0.1,\ \omega = 0.1$

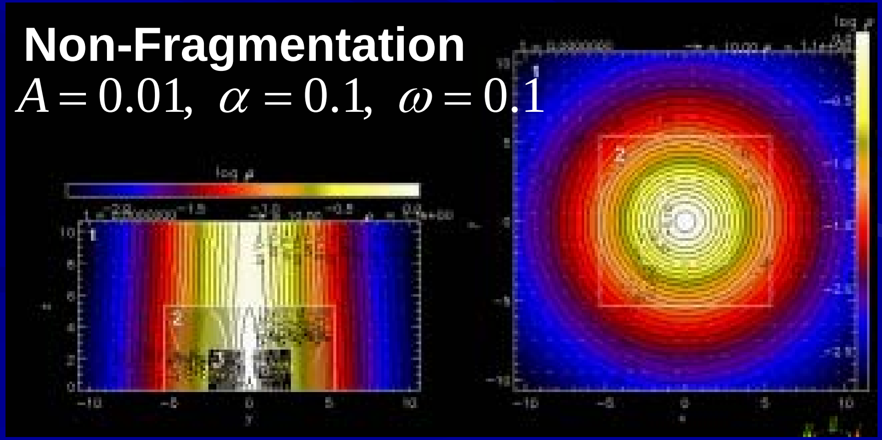

B-Ω Flux-Spin Relation

Machida et al. 2005a,b

--Evolutionary Path--

$$B_c/(8\pi c_s^2\rho_c)^{1/2} - \Omega_c/(4\pi G\rho_c)^{1/2}$$

Support deficient.
➔ Spherical collapse.

$$B_c \propto \rho_c^{2/3} \rightarrow B_c R^2 = \text{const}$$
$$\Omega_c \propto \rho_c^{2/3} \rightarrow \Omega_c R^2 = \text{const}$$
$$\Downarrow$$
$$\Omega_c/\rho_c^{1/2} \propto B_c/\rho_c^{1/2} \propto \rho_c^{1/6}$$
$$\Omega_c/B_c \approx \text{const}$$

Magnetic braking

$$B_c/\rho_c^{2/3} \approx \text{const}$$
$$\Omega_c/\rho_c^{2/3} \downarrow \quad \text{J-loss}$$
$$B_c/\Omega_c \uparrow$$

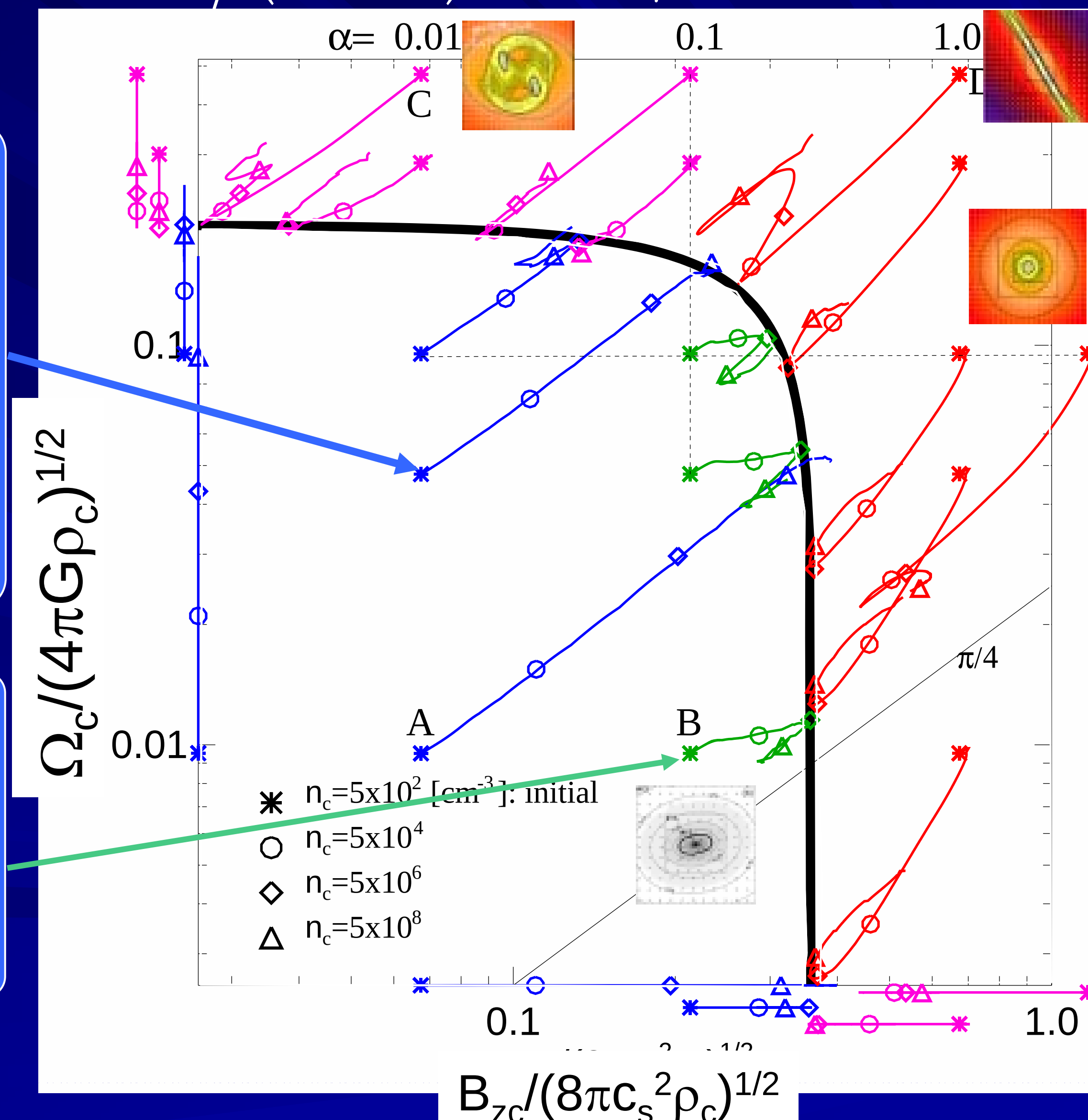

B-Ω Flux-Spin Relation

--Evolutionary Path--

$B_c/(8pc_s^2 r_c)^{1/2}$ - $W_c/(4pGr_c)^{1/2}$

Support sufficient

➔Disk formation

B_c ; const r_c Z

W_c ; const

→move left-down

$W_c / r_c^{1/2}$ オ $B_c / r_c^{1/2}$ オ $r_c^{-1/2}$

➔Radial collapse

B_c / s_c ; const ←frozen-in

W_c / s_c ; const ←conserve J

$s_c / r_c^{1/2}$; const ←self-grav. disk

→move slightly

Magnetic braking

B_c / W_c Z

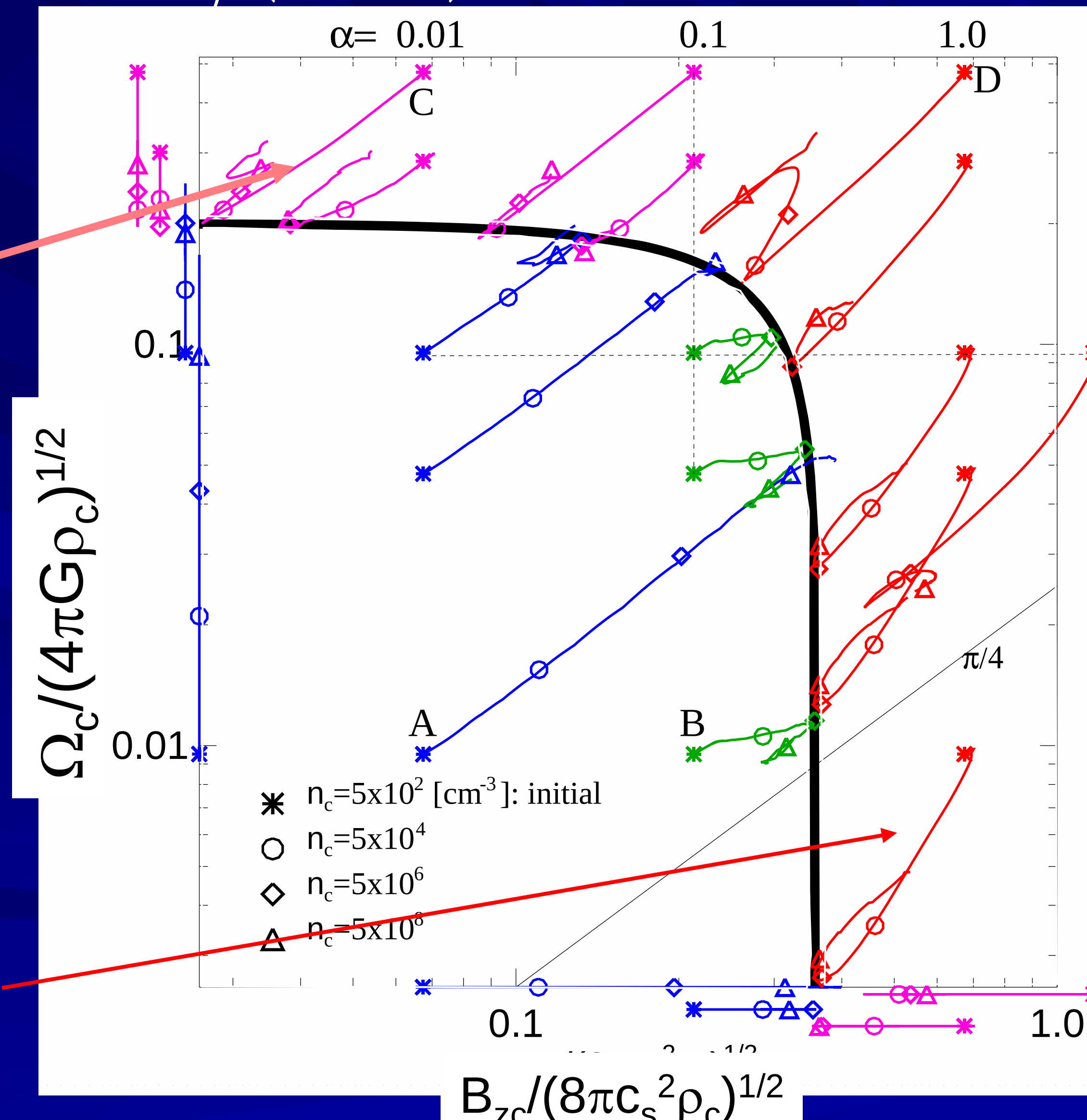

B-Ω Flux-Spin Relation

--Evolutionary Path--

- In the isothermal run-away collapse, contraction proceeds self-similarly or solution converges to a family of self-similar solutions.
- All the models converge to a line as

$$\frac{B_c^2}{(0.36)^2 8\pi c_s^2 \rho_c} + \frac{\Omega_c^2}{(0.2)^2 4\pi G \rho_c} = 1 \qquad \text{empirical}$$

- There exists a balance between B-field, centrifugal force, thermal pressure and gravity.

1. We know both the <u>evolutionary path</u> and <u>fragmentation condition</u> $\varepsilon_{ob}>3$ or $\Omega_c/(4\pi G\rho_c)^{1/2}>0.2$.
2. This gives a diagnosis of a cloud: fragments in the adiabatic stage or remains single ?

For the adiabatic core to fragment, it must rotate fast enough.

Large symbols initial states

Fragmentation

No fragmentation

Small symbols Adiabatic core

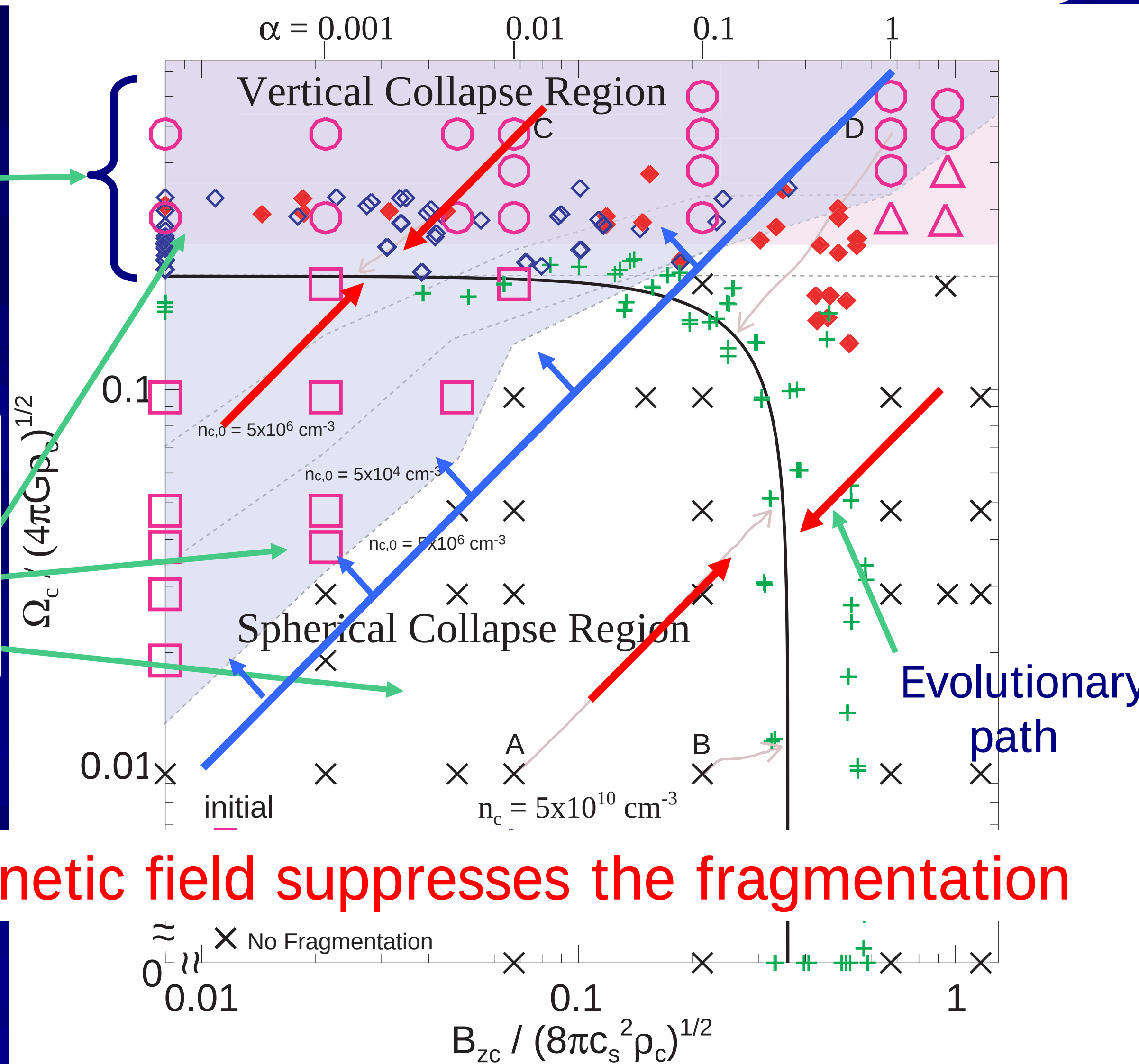

Magnetic field suppresses the fragmentation

To Fragment

$$\frac{\Omega_0}{B_0} > \frac{G^{1/2}}{2^{1/2} c_s} \sim 3\times 10^{-7}\,\mathrm{yr^{-1}}\,\mu\mathrm{G^{-1}} \left(\frac{c_s}{90\,\mathrm{m s^{-1}}}\right)^{-1}$$

Prestellar core L1544

$v_f \sim 0.09\,\mathrm{km\,s^{-1}}\ @\ r = 15000\,\mathrm{AU}$ Ohashi et al (1999)

$\Rightarrow \Omega_0 \sim 1.3\times 10^{-6}\,\mathrm{yr^{-1}}$

$v_f \sim 0.14\,\mathrm{km\,s^{-1}}\ @\ r = 7000\,\mathrm{AU}$ Williams et al (1999)

$\Rightarrow \Omega_0 \sim 4.2\times 10^{-6}\,\mathrm{yr^{-1}}$

$B_0 \sim +11 \pm 2\,\mu\mathrm{G}$ Zeeman splitting Crutcher & Troland (2000)

$$\Rightarrow \frac{\Omega_0}{B_0} \sim (1.2 - 3.8)\times 10^{-7}\,\mathrm{yr^{-1}}\,\mu\mathrm{G^{-1}}$$

Marginal!!

Measurement both Ω and B at the same density
➔ future forecast!

Alignment of Outflow and Magnetic Field

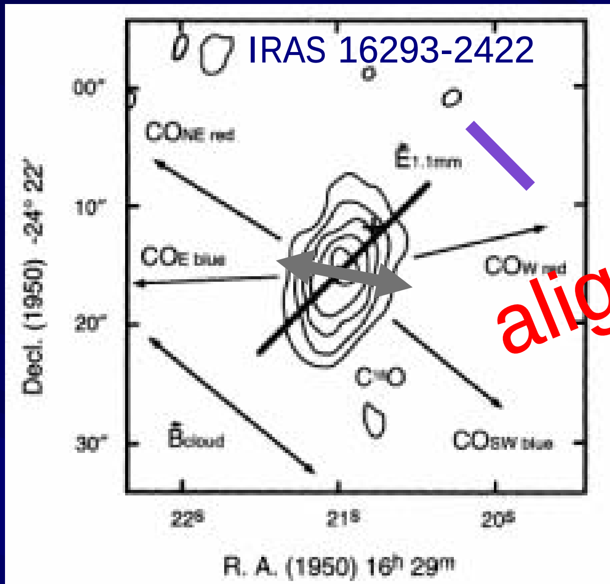

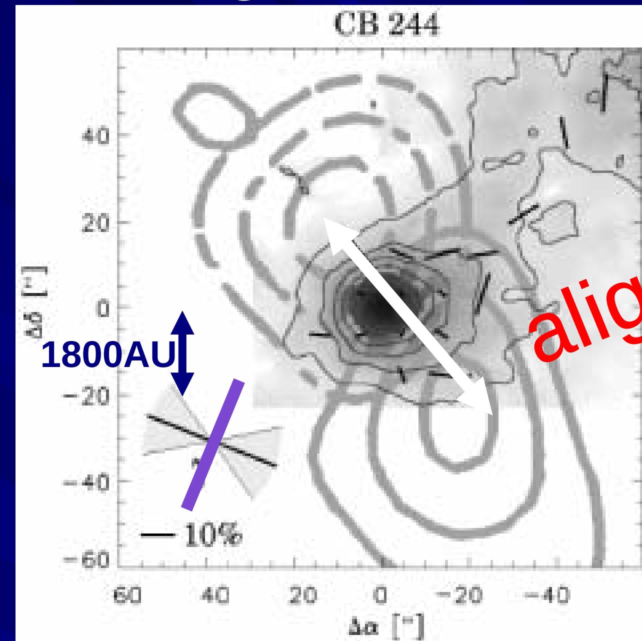

Wolf et al (2003)

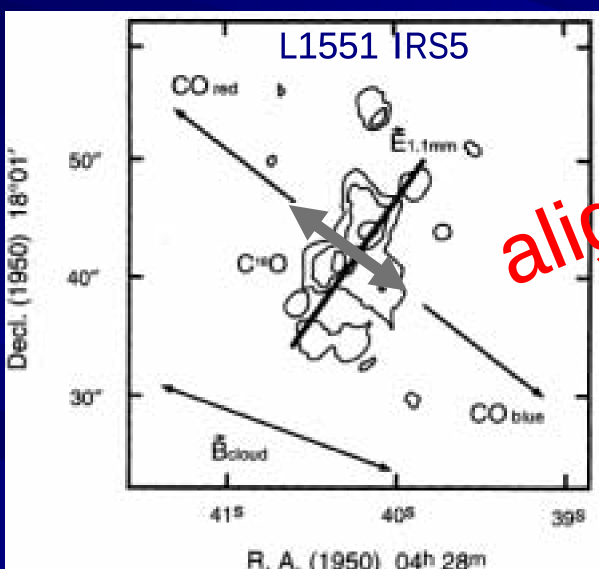

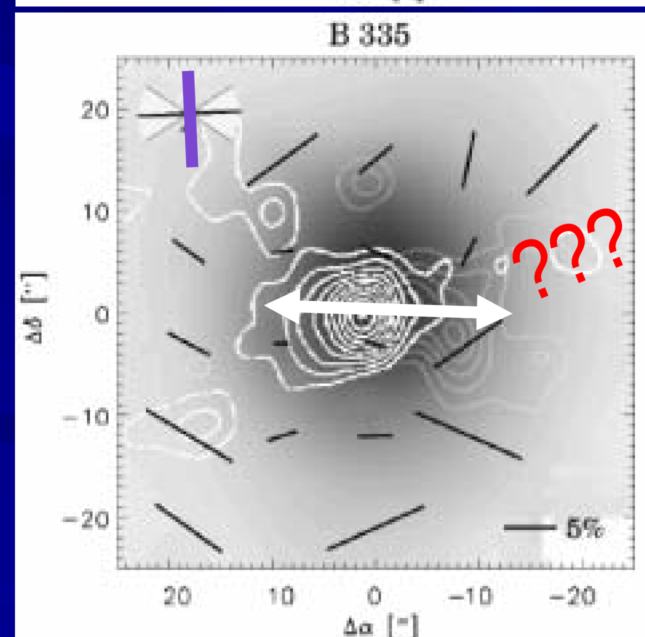

Outflow

Magnetic field

Tamura et al (1995) 1mm radio polarization

Polarization of thermal dust emission map SCUBA 850μm

Miss-aligned case

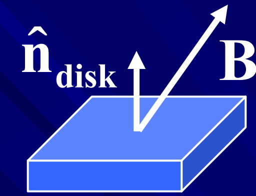

$B_{cp} \equiv \mathbf{B}\cdot\hat{\mathbf{n}}_{disk}$ $\Omega_{cp} \equiv \mathbf{\Omega}\cdot\hat{\mathbf{n}}_{disk}$

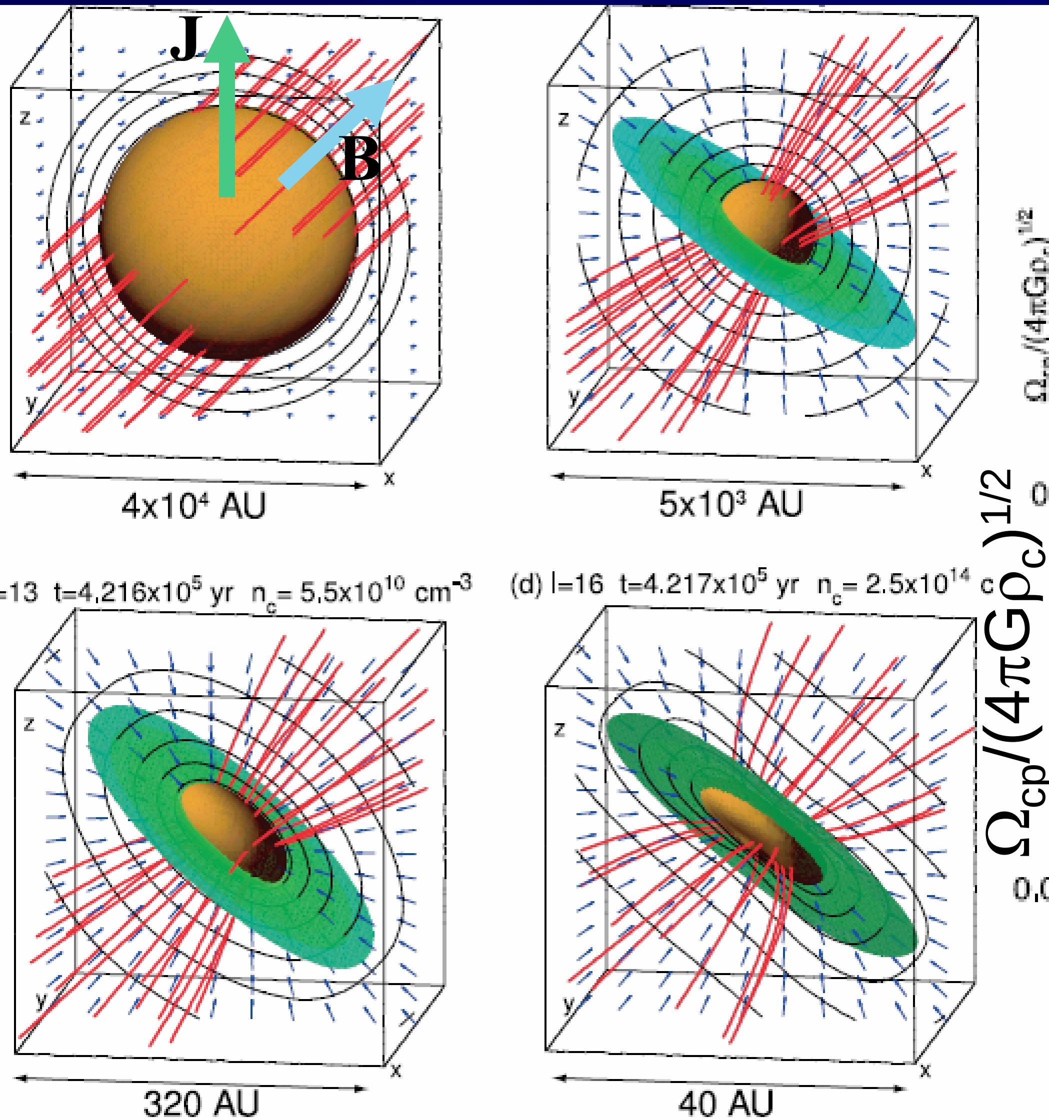

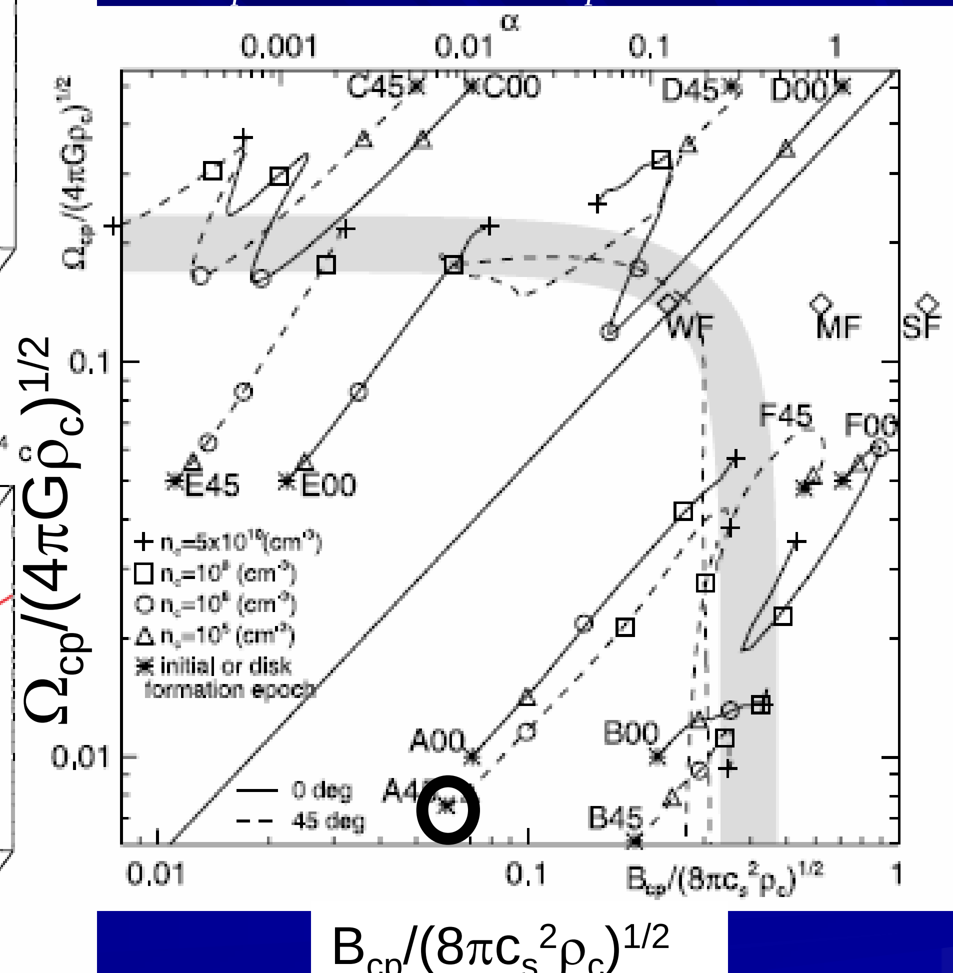

$\alpha = 0.01,\ \omega = 0.01$ Evolution is understood by the spin-flux relation.

Direction of the Disk

- Rotation-dominant:
  - disk ∧ **J**
- Magnetic-dominant:
  - disk ∧ **B**
- Boundary is given

$$\frac{W_0}{B_0} = 0.39\frac{G^{1/2}}{c_s}$$

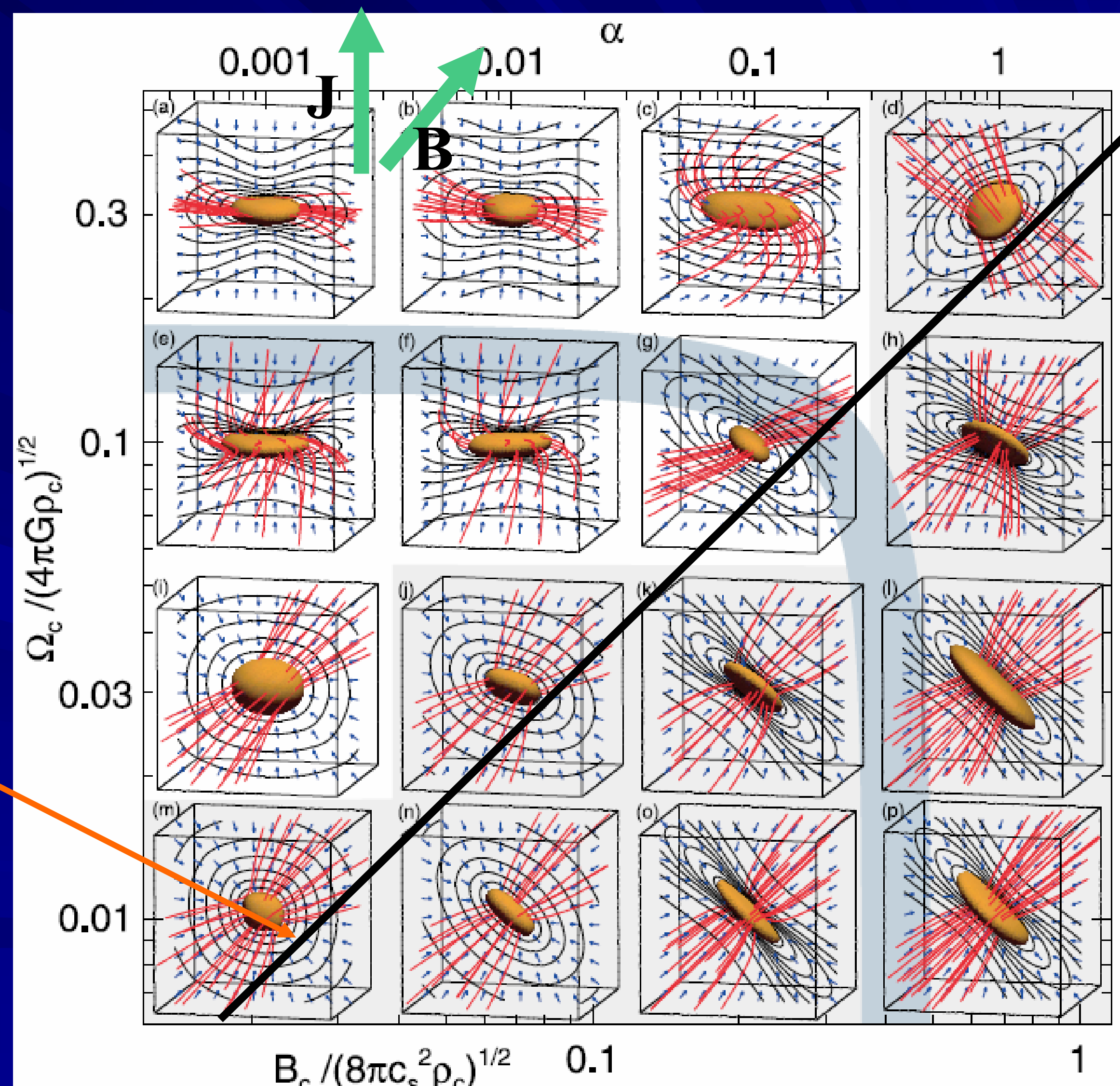

Disk, B Field and Rotation in Different Scales (Final state)

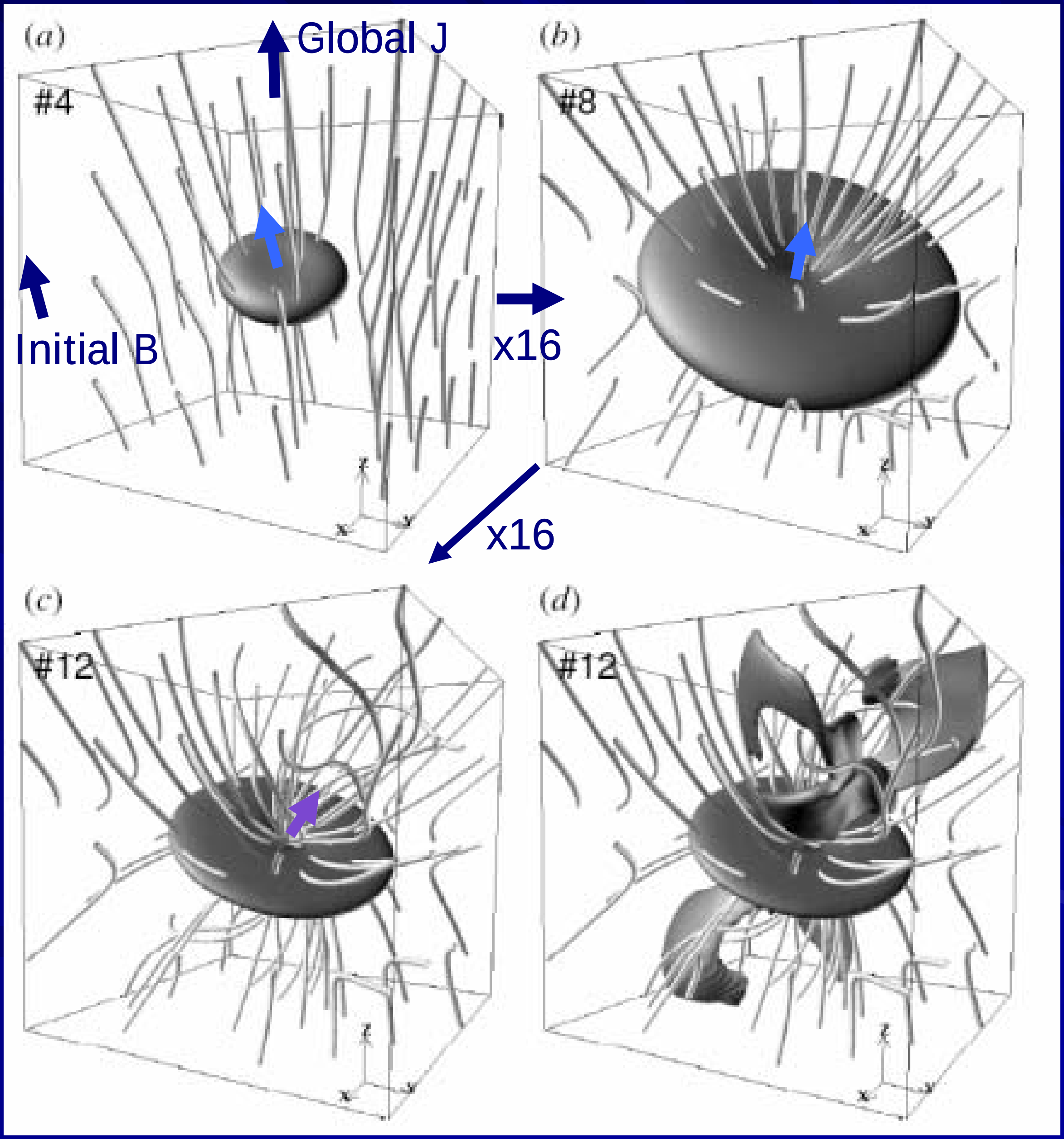

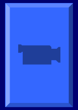

Disk oriantation, local B, and local J change their directions according to the scale.

Matsumoto & T. 2004

Qualitative

Summary for Part 1

- Magnetic field (B) and angular momentum (J) play cooperatively a role to form e.g. outflows.
- B reduces the power of J to form fragmentation.
- Disk is formed either by J or B depending on the dominant force: J or B.

Evolution of a Rotating First Core

Saigo & Tomisaka (2006, ApJ, 645, 381-394)

Saigo, Matsumoto, Tomisaka (2006, in prep.)

- I have showed that B-field controls the angular momentum of the first core.
- Fragmentation develops quickly in a hydrostatic state (first core) rather than in a contracting circumstance (runaway phase)
- Fragmentation in a first core may bring binary or multiple stars.
  ←binaries are more popular than single stars.
- Ideal MHD should be reconsidered.

Temp-density relation of IS gas. (Tohline 1982)

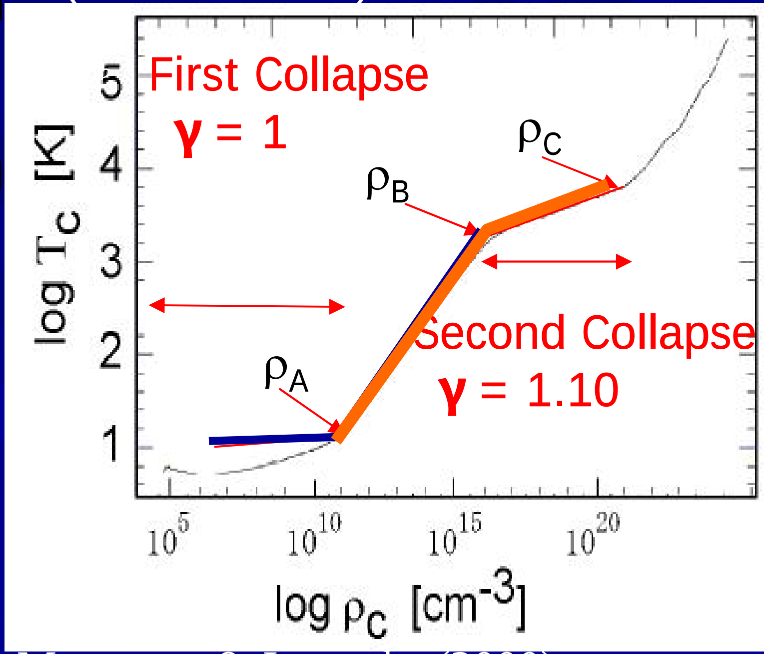

Masunaga & Inutsuka (2000)

Hydrostatic Equilibrium

- Hydrostatic Axisymmetric Configuration for Barotropic Gas

$$\left(\rho r \Omega^2, 0, 0\right) - \nabla P - \rho \nabla \psi = 0,$$

$$\Delta \psi = 4\pi G \rho$$

$$p \approx \begin{cases} K_1 \rho^{7/5} \quad \mathrm{K} & (\rho \le \rho_{dis}) \\ K_2 \rho^{1.1} \quad \mathrm{K} & (\rho > \rho_{dis}) \end{cases}$$

dissociation density

- Angular Momentum Distribution
  - same as a uniform-density sphere with rigid-body rotation
  - total mass M_{core} and total ang. mom. J_{core}

$$j(M(R)) = \frac{5}{2}\left(\frac{J_{core}}{M_{core}}\right)\left\{1 - \left(1 - \frac{M(R)}{M_{core}}\right)^{2/3}\right\}$$

- Self-consistent Field Method (SCF) Hachisu(1986), Tohline, Durisen

$$\left(M_{core}, J_{core}\right) \to \rho_c$$

  - to understand the evolution of first core

$$\left(\rho_c, M_{core}\right) \to J_{core}$$

Examples of Hydrostatic Configuration

Ω Z M Z

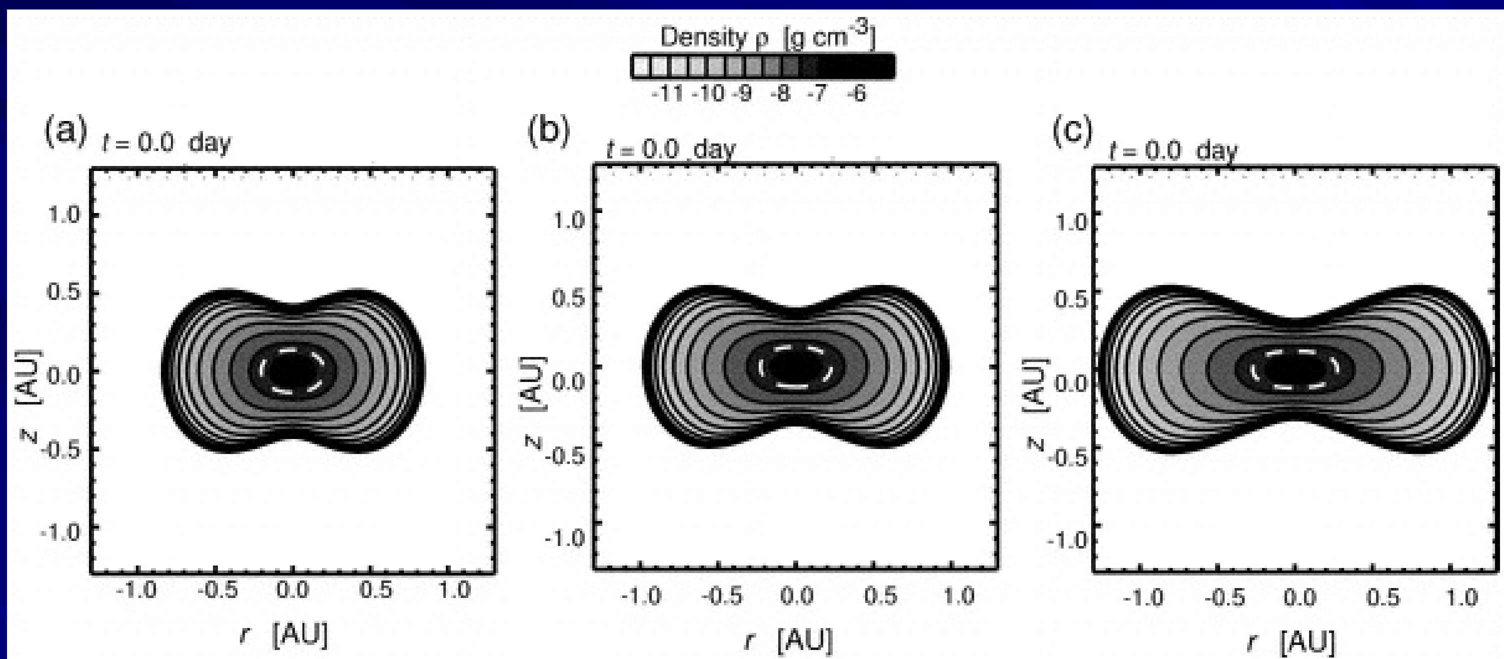

Three models have the same central density $\rho_c = 4\rho_{diss}$, but different angular momenta as 2.25×10^{49} (left), 4.18×10^{49} (middle), and 9.99×10^{49} g cm^2 (right), and masses as 2.77×10^{31} (left), 3.45×10^{31} (middle), and 4.97×10^{31} g (right).

Mass-Density Relation ($\Omega = 0$)

- Below $\rho \lesssim \rho_{dis}$ mass increases with central density ρ_c.
  - Mass is prop. to Jeans mass
    $$M_J \propto T^{3/2}\rho^{-1/2} \propto \rho^{1/10}$$
    (Chandrasekhar 1949)
  - Mass accretion drives the core from lower-left to upper-right.

$\rho_{dis} = 5\times10^{-8}\,\mathrm{gcm}^{-3}$

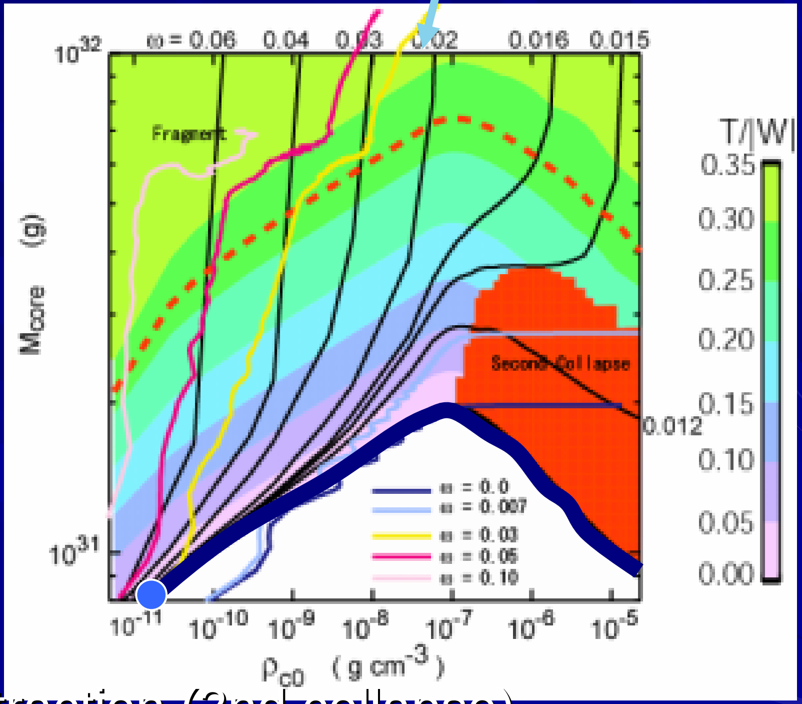

- Above $\rho \gtrsim$ a few ρ_{dis} mass decreases due to soft EOS.
  - Further accretion destabilizes the cloud and drives dynamical contraction (2nd collapse).
- Maximum mass of the 1st core is 0.01 $M_\odot$.

Hydrodynamical Simulation

- run-away (1st collapse)→ 1st core
  - 1st core grows by mass accretion from contracting envelope.
- Initial Condition
  - Bonnor-Ebert sphere (+ envelope (R~50,000AU))
  - $n_c \sim 10^4 H_2 cm^{-3}$, T=10K
  - Rotation $\omega = \Omega t_{ff} = 0 \sim 0.3$
  - increase the BE density by 1.1~8 times
  - Perturbations m=2 and m=3 $\delta\rho/\rho$=10%
- Numerical method
  - HD nested grid
  - barotropic EOS

Non-rotating cloud

- density $\rho_c < \rho_{dis}$, Mcl increases with ρ_c.
  - Jeans mass
    $$M_J \propto T^{3/2} \rho^{-1/2} \propto \rho^{1/10}$$
  - Evolution is driven by accretion.
- At $\rho_c > 2\rho_{dis}$, soft EOS makes Mcl decrease.
  - dynamical contraction (2nd collapse)
- maximum mass of a 1st core is equal to ~0.01 $M_\odot$.

$$\rho_{dis} = 5 \times 10^{-8}\,\mathrm{g\,cm^{-3}}$$

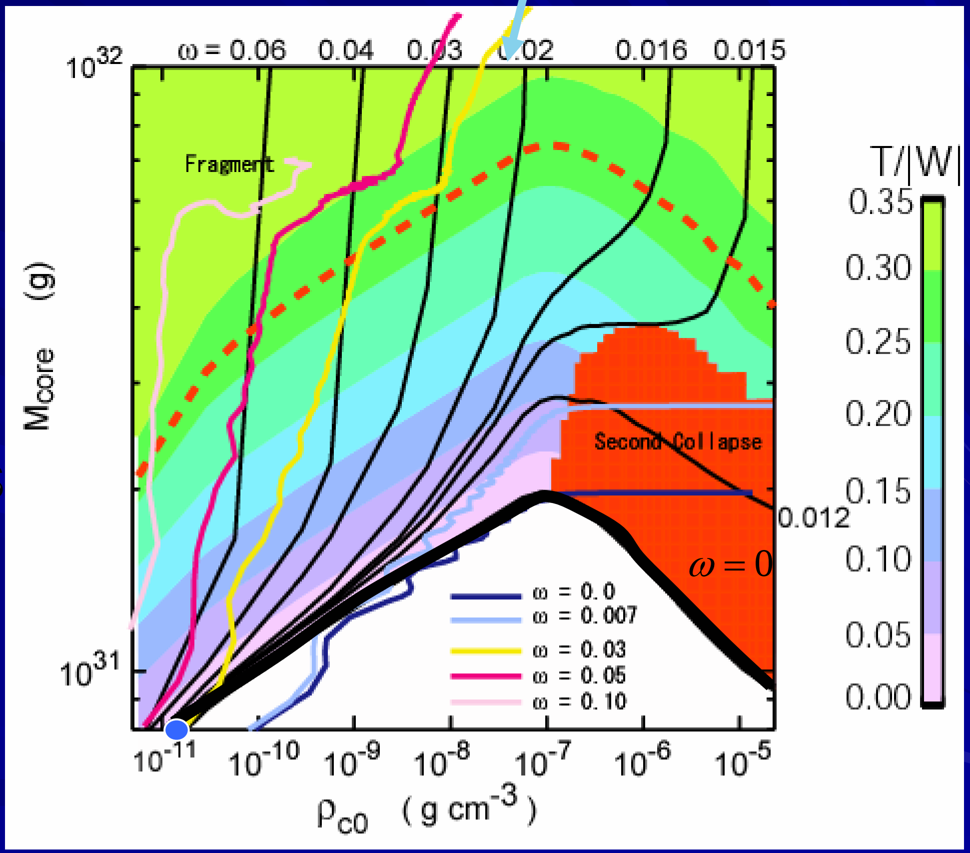

Non-rotating model

1. Unless the cloud is much more massive than the B-E mass, the first core evolves to follow a path expected by quasi-hydrostatic evolution.

2. Maximum mass of a first core is small ~0.01M$_{\odot}$.

3. Quasi-static evolution gives a good agreement with HD result.

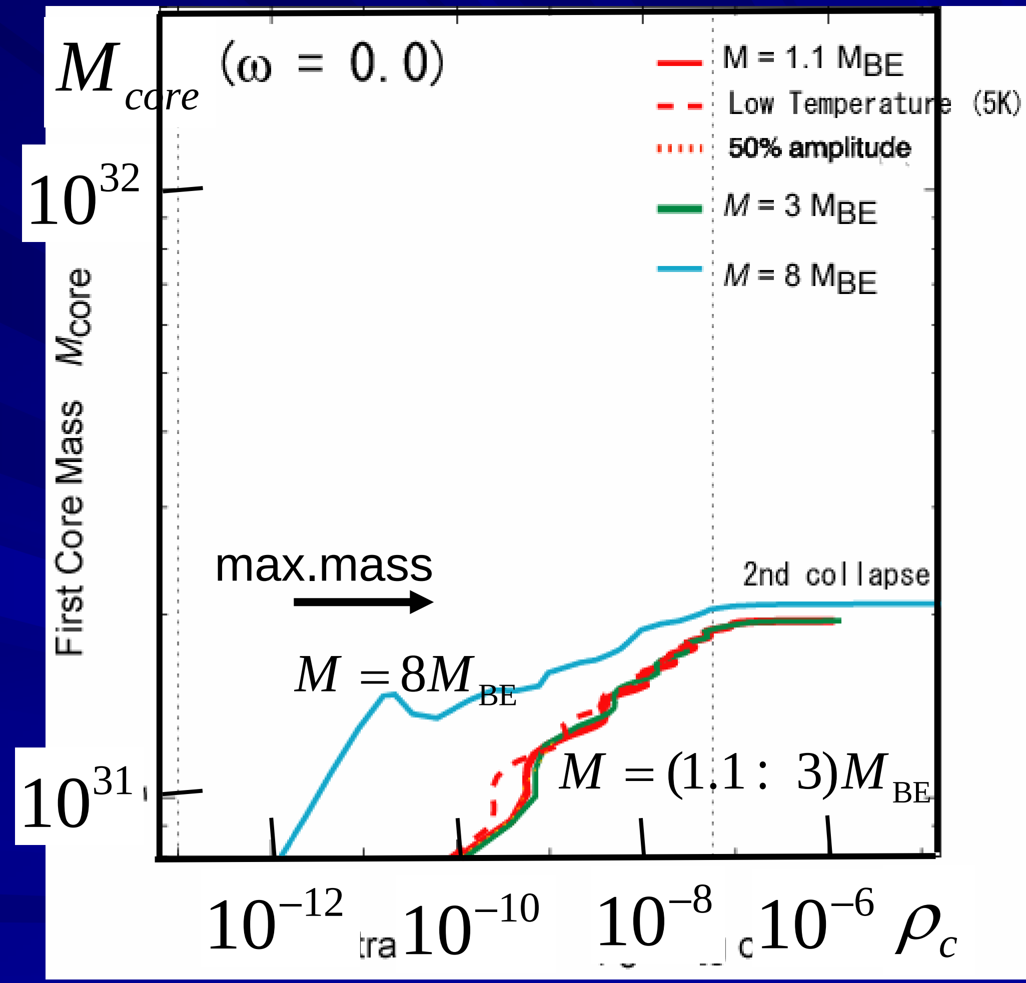

Mass-Density Relation ($\Omega > 0$)

- rotation rate of parent cloud

$$\omega = \frac{j}{M}\left(\sqrt{2}c_s / G\right)$$

- ω<0.015
  - similar to non-rot. case.
  - second collapse

- ω>0.015
  - Mass increases much well below $\rho_c = \rho_{dis}$

$\rho_{dis} = 5\times10^{-8}\,\mathrm{gcm}^{-3}$

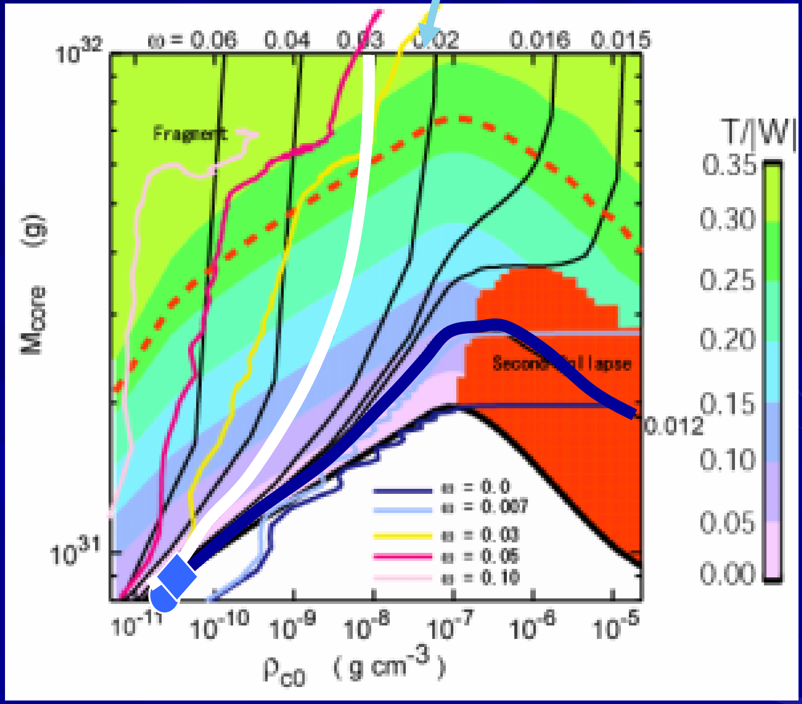

Rotating Cloud (ω=0.05)

- First, the 1st core increases its mass (upwardly in M_{cl}-ρ_c plane).
  - follows a hydrostatic evolution path.
  - Shape: round spherical disk.

- Then, the first core begins to contract (rightward in the plane)
  - This phase, spiral arms appear.
  - J is transferred outwardly.

- Core+disk continues to contract.

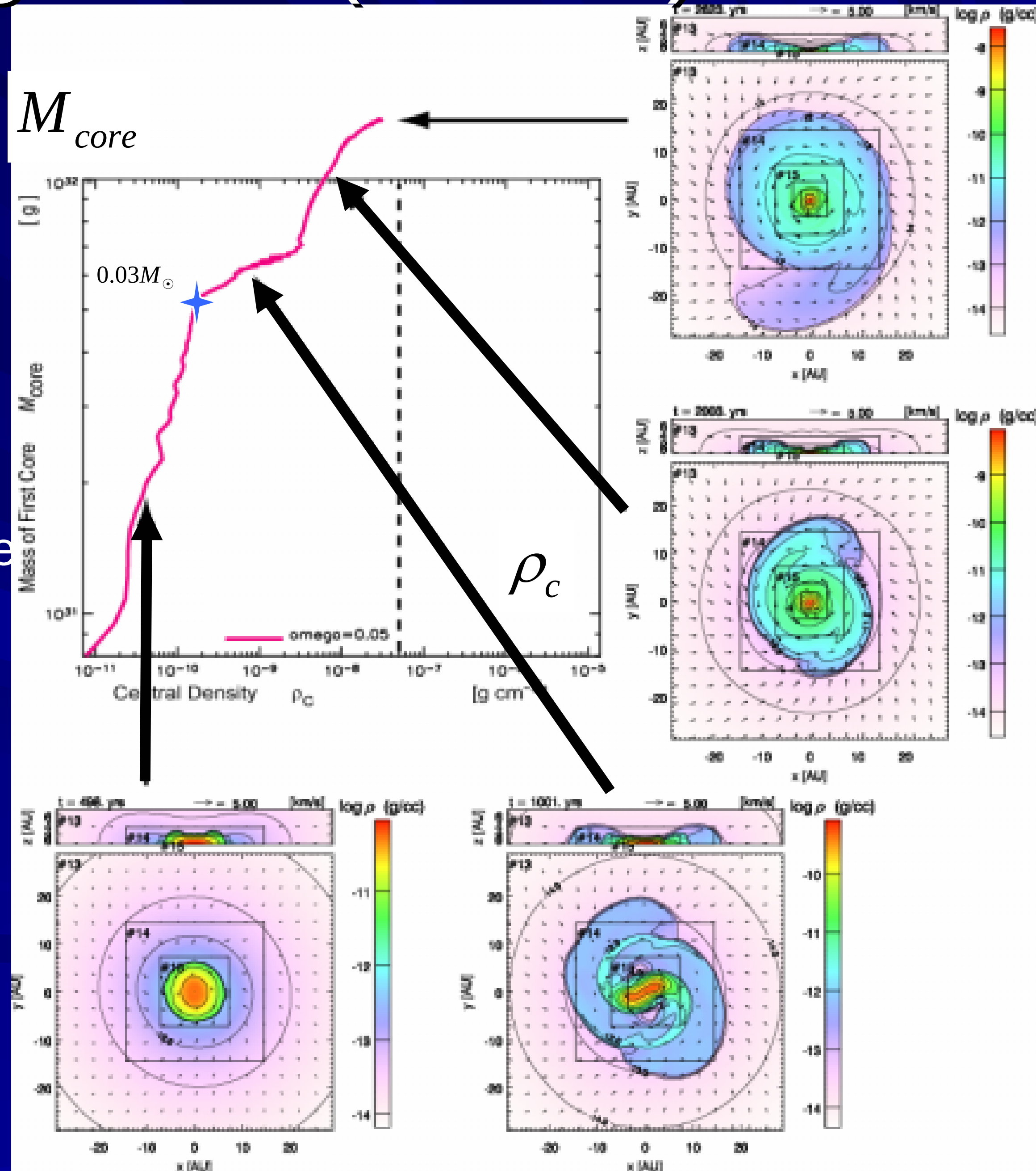

Comparison with previous simulations

- Bate (1998)
  - SPH simulation
  - ω=0.08
  - spiral → transfer J
- Matsumoto, Hanawa (2003)
  - Nested Grid Eulerian Hydrodynamics
  - ω=0.03
    - spiral
  - ω=0.05
    - spiral
    - fragmentation

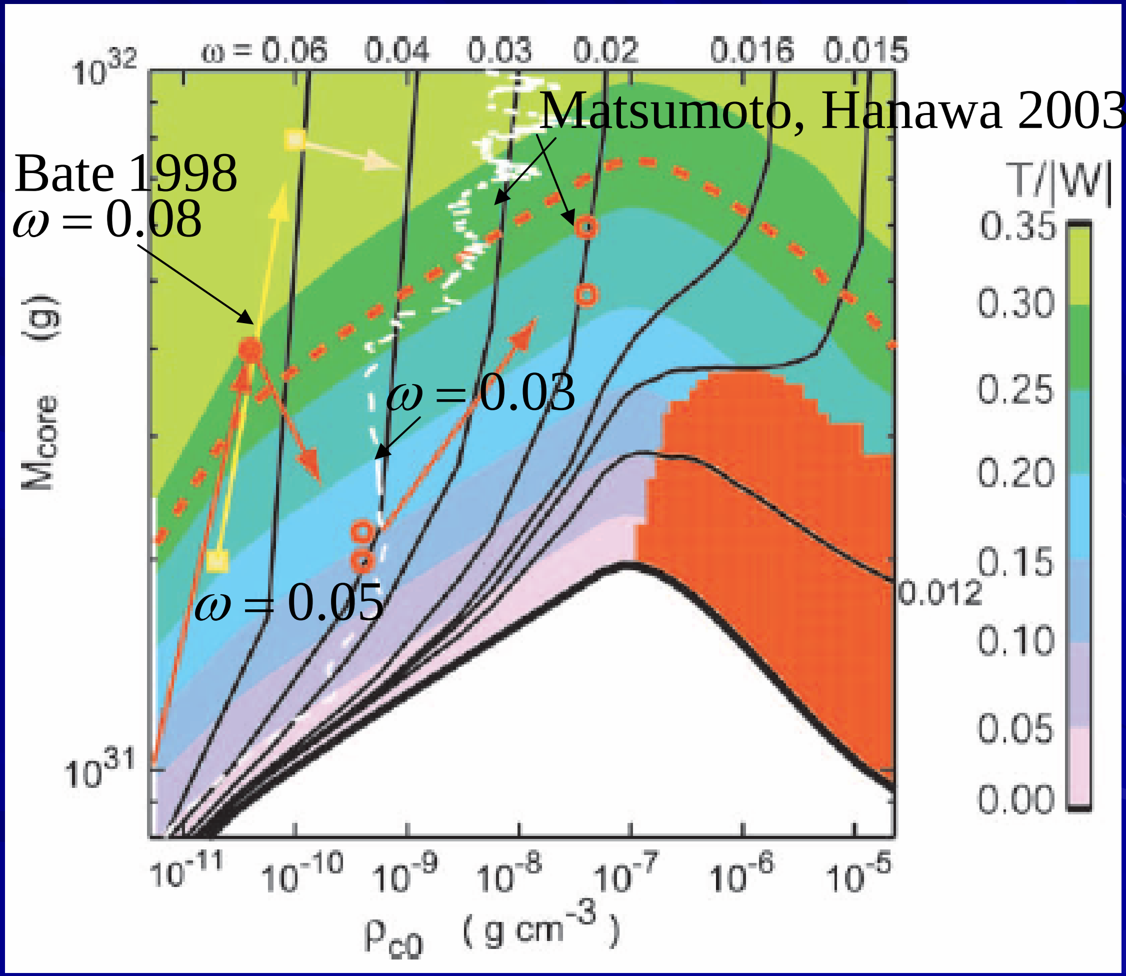

Nonaxisymmetric instability

- Rotational-to-gravitational energy ratio: *T*/|*W*|
  - A polytropic disk with *T*/|*W*|>0.27 (γ=5/3) is dynamically unstable under a wide range of conditions (γ=5/3: Pickett et al. 1996; γ=7/5, 9/5, 5/3 Imamura et al. 2000)
- *T*/|*W*| increases with mass accretion.
- After *T*/|*W*| exceeds the critical value,
  - nonaxisymmetric instability grows.
  - Angular momentum is transferred outwardly.
  - This may stabilize the disk again.

$\rho_{dis} = 5\times10^{-8}\,\mathrm{g cm}^{-3}$

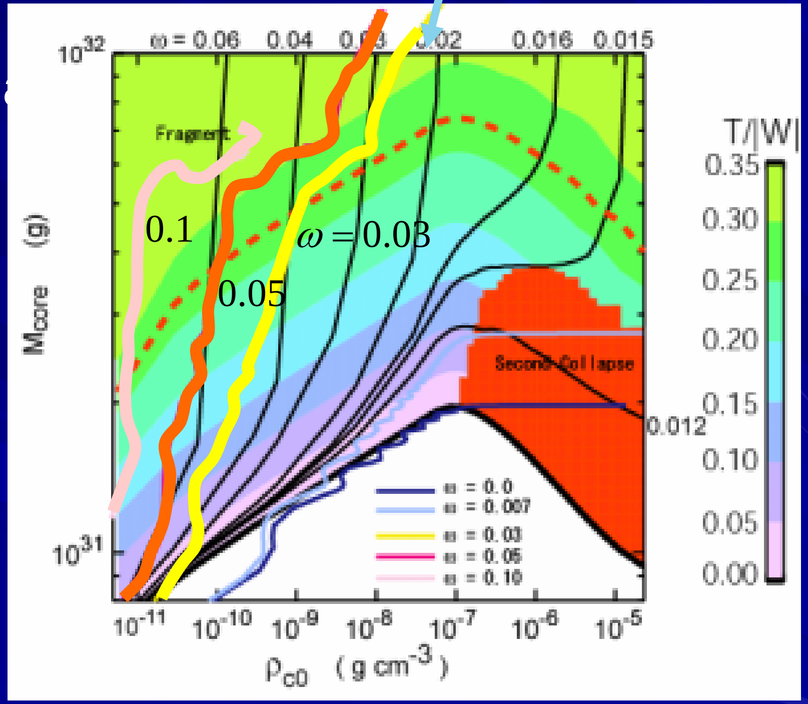

Rotating Cloud (ω=0.05)

- Evolution depends on the initial mass.
  - – $M \sim M_{BE}$:
    - Follow quasihydrostatic evolution
  - – $M >> M_{BE}$:
    - evolution depends on its initial condition.

$\rho_{dis} = 5\times10^{-8}\,\mathrm{g\,cm^{-3}}$

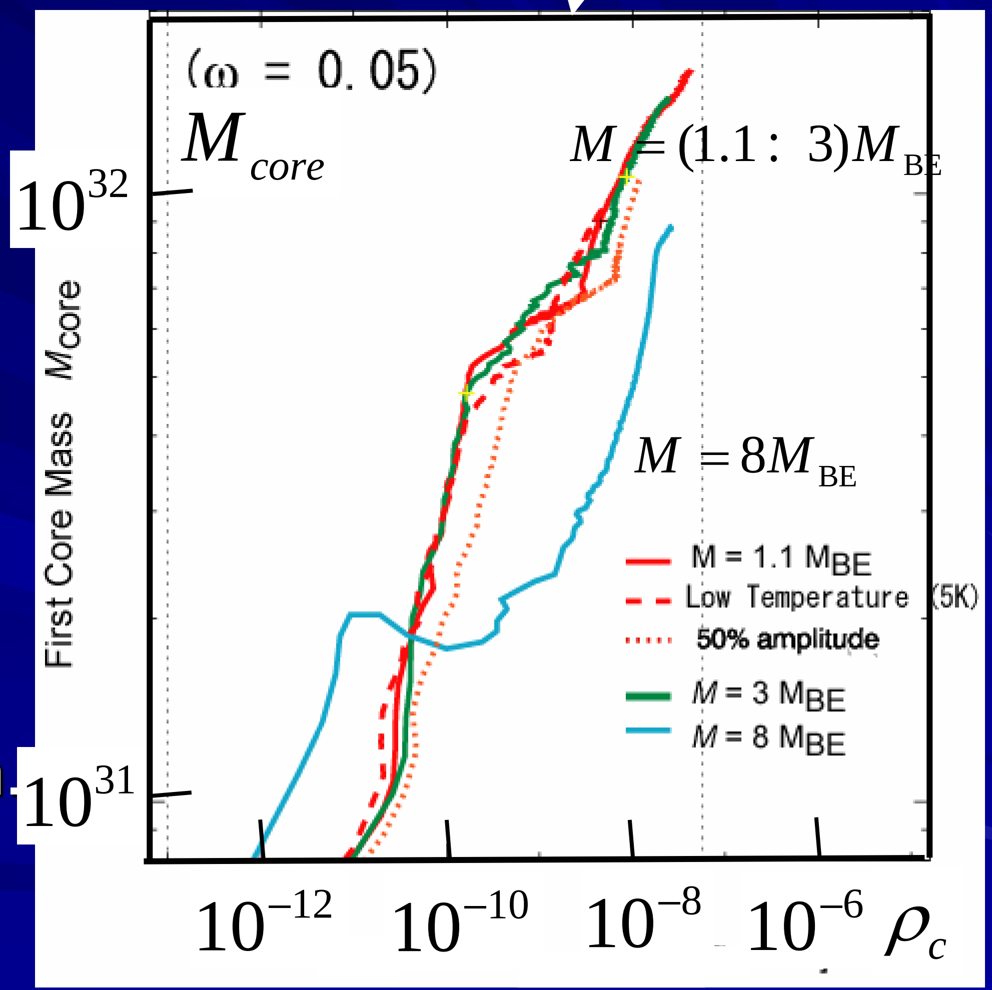

Fragmentation

- In a fast rotating cloud, fragmentation (more than 2 fragments) is observed in the 1st core.
- This occurs after non-axisymmetric instability is triggered.
-

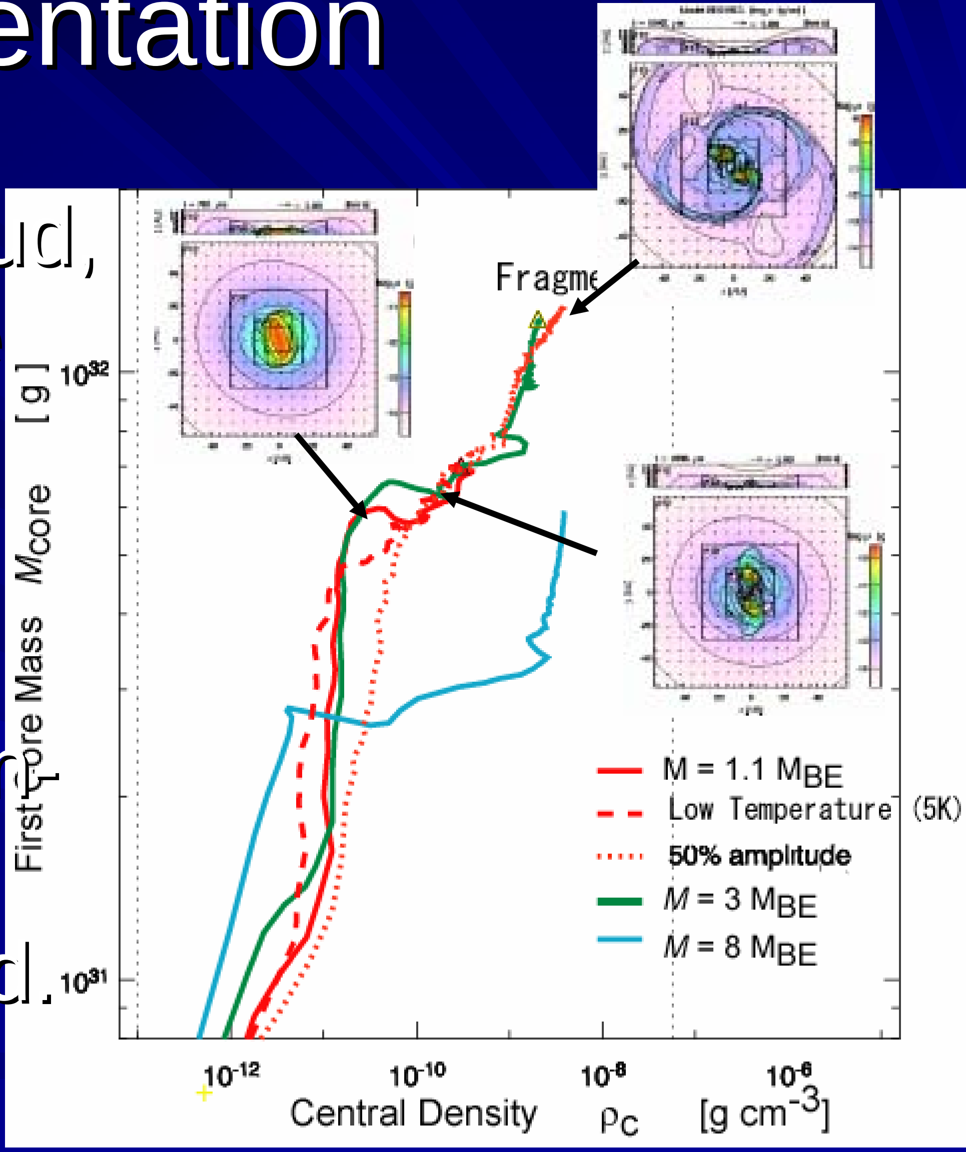

Typical Rotation Rate

- NH_3 cores ($n \sim 3\ 10^4 cm^{-3}$) Goodman et al (1993)

$$\Omega\ ;\ (0.3-2)\times 10^{-6}\,\text{rad yr}^{-1}$$

$$\tau_{ff} = \left(\frac{3\pi}{32G\rho}\right)^{1/2}\ ;\ 2\times 10^{5}\,\text{yr} \longrightarrow \omega\ ;\ 0.06-0.4$$

- N_2H^+ cores ($\sim 2\ 10^5 cm^{-3}$) Caselli et al. (2002)

$$\Omega\ ;\ (0.5-6)\times 10^{-6}\,\text{rad yr}^{-1}$$

$$\tau_{ff} = \left(\frac{3\pi}{32G\rho}\right)^{1/2}\ ;\ 8\times 10^{4}\,\text{yr} \longrightarrow \omega\ ;\ 0.04-0.5$$

Luminosity of the First Core

$$L = -\frac{dE_{tot}}{dt} = -\frac{d}{dt}\left(W + E_{kin} + E_{th}\right)$$

3D simulation

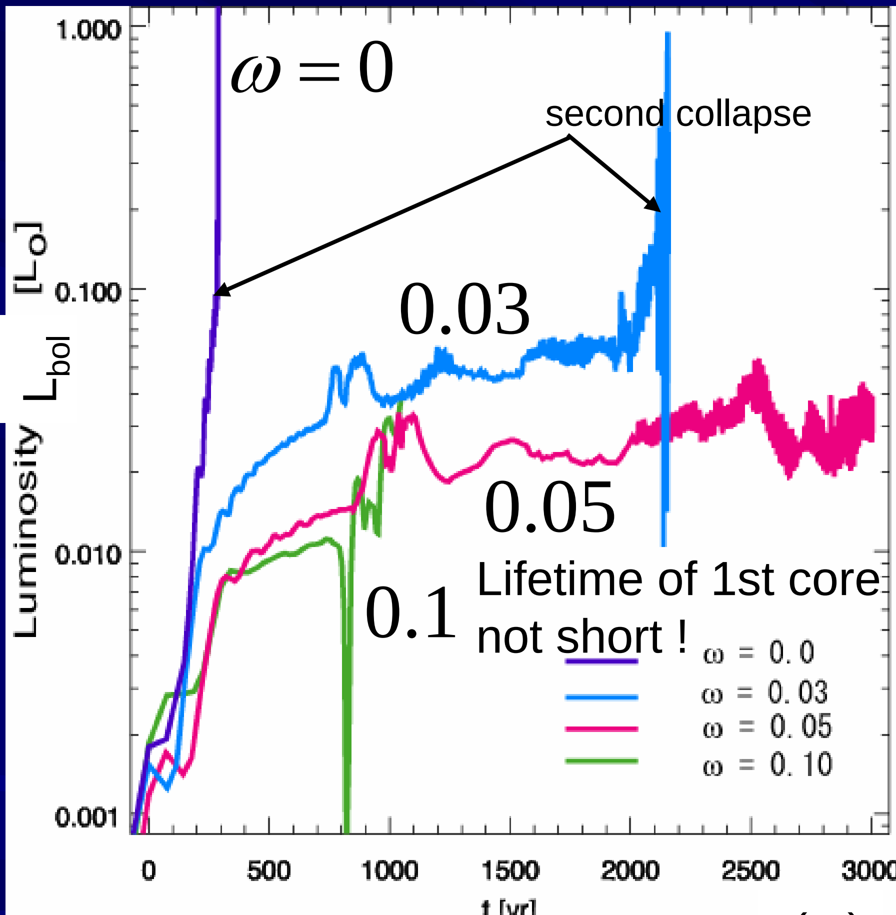

Quasi-static evolution

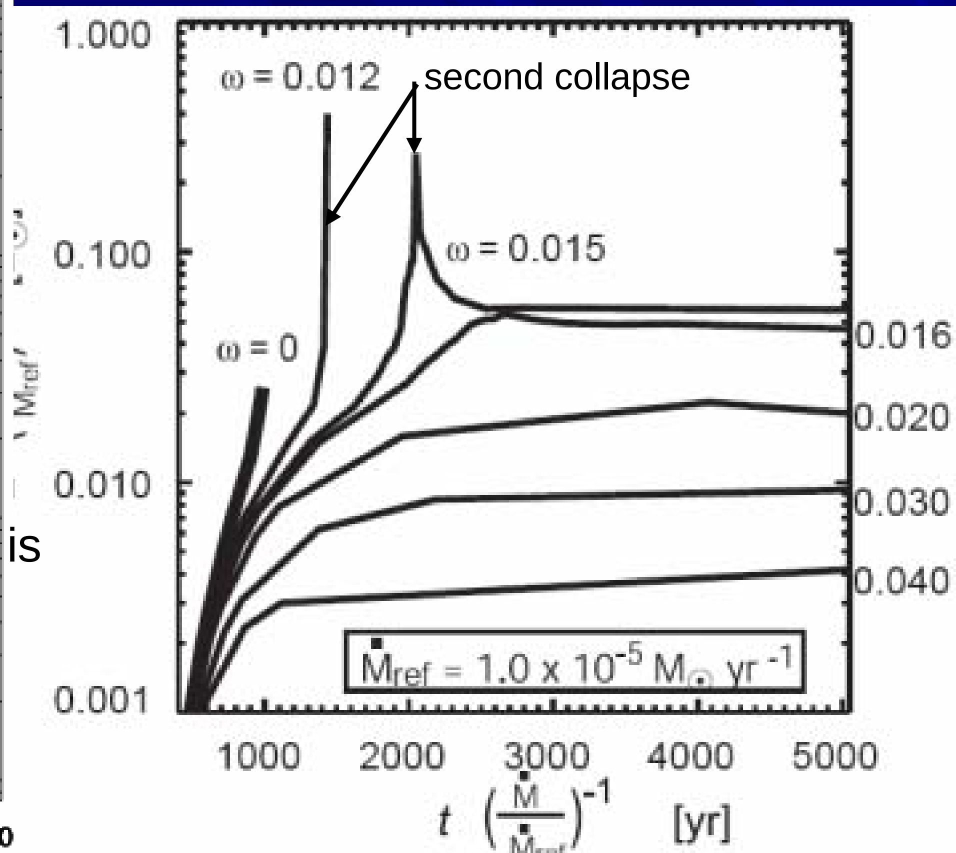

L is a decreasing function of ω.
$\dot{M} \sim 2\times10^{-5} M_\odot \mathrm{yr}^{-1}$
$L \sim (3-5)\times10^{-2} L_\odot$

Absolute value L and timescale are obtained after $\dot{M}$ is given. $L \propto \dot{M}$ $t \propto \dot{M}^{-1}$

Mass Accretion Rate

- Mass accretion rate is between the LP solution and a SH disk solution.
- Much higher than that expected for SIS.

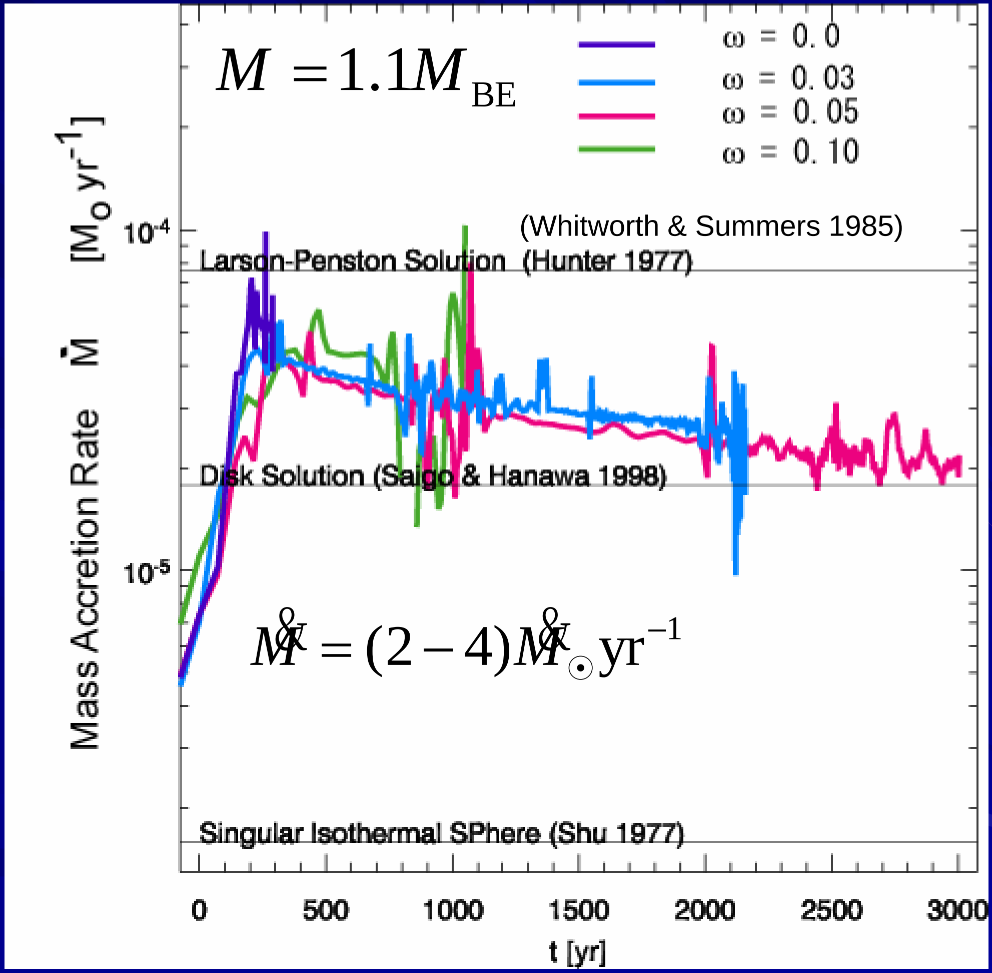

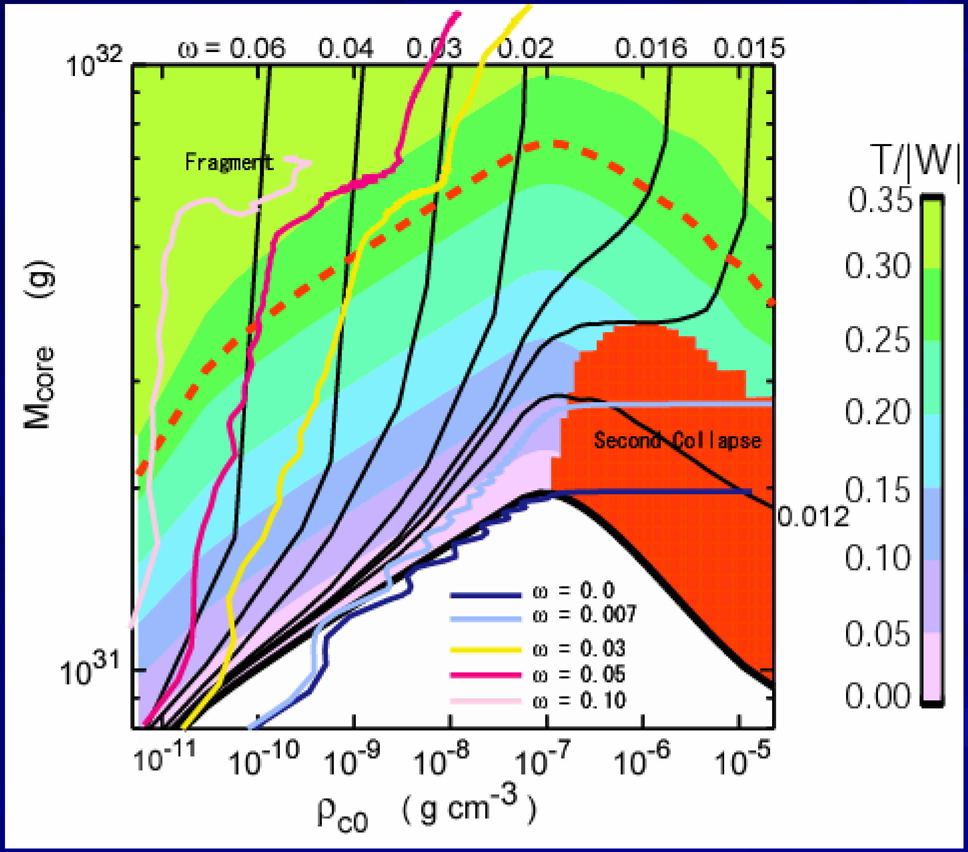

ω = 0.06
0.04
0.03
0.02
0.016
0.015
0.012
Fragment
Second Collapse
10^{32}
10^{31}
M_{core} (g)
10^{-11}
10^{-10}
10^{-9}
10^{-8}
10^{-7}
10^{-6}
10^{-5}
ρ_{c0} (g cm^{-3})
ω = 0.0
ω = 0.007
ω = 0.03
ω = 0.05
ω = 0.10
T/|W|
0.35
0.30
0.25
0.20
0.15
0.10
0.05
0.00

Summary

- The evolution of a 1st core is well described with the quasi-static evolution.
- Slow (or no) rotation model exhibits the second collapse (ω<0.015).
  - Maximum mass of the 1st core ~0.02 $M_{\odot}$ (ω=0.015).
- Rotating cloud with ω>0.015, the 1st core contracts slowly.
  - After T/|W|>0.27, a dynamical nonaxisymmetric instability grows and spiral pattern appears.
  - Gravitational torque transfers the angular momentum outwardly.
  - The 1st core contracts further.
- In a rotating cloud with ω>0.1, we found the fragmentation of the 1st core.